NASA Technical Paper 2083

November 1982

Correlation and Assessment of Structural Airplane Crash Data With Flight Parameters at Impact

Huey D. Carden

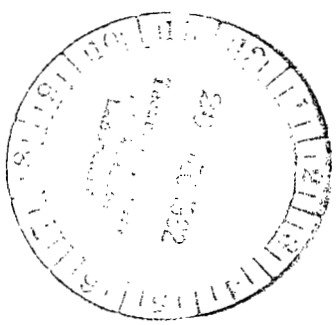

NASA

NASA
Technical
Paper
2083

1982

Correlation and Assessment of Structural Airplane Crash Data With Flight Parameters at Impact

Huey D. Carden
Langley Research Center
Hampton, Virginia

NASA
National Aeronautics
and Space Administration

**Scientific and Technical
Information Branch**

SUMMARY

An analysis has been made of crash-deceleration pulse data from a crash-dynamics program on general aviation airplanes and from transport crash data available in the literature. This crash-dynamics program has been a joint effort since 1973 by the National Aeronautics and Space Administration (NASA) and the Federal Aviation Administration (FAA). The purpose of the analysis was to correlate and assess structural airplane crash data with flight parameters at impact.

In the analysis, assumptions made to simplify the complex crash scenario led to uncoupled equations for the normal and longitudinal floor impulses (deceleration multiplied by duration) in the cabin area of the airplane. Analytical expressions for structural crushing during impact and for the airplane horizontal slide-out were also determined. Good agreement was found between experimental and analytical data for general aviation and transport airplanes over a relatively wide range of impact parameter.

Since the analysis yielded only the product of the deceleration and duration (not amplitudes), two possible applications are presented: a postcrash evaluation of crash parameters and an assumed crash scenario.

Although the values of airplane crash-test parameters associated with the data of this report cannot be considered comprehensive for all crash situations encountered by light airplanes, it is believed that these values are typical of a large percentage of crash situations. Thus, these data are believed to be of general significance regarding the assessment of expected loads at the seat/occupant structural interface for general aviation airplanes during serious but potentially survivable crashes.

INTRODUCTION

During recent years, increased emphasis has been focused on causes of passenger injuries and fatalities resulting from severe, but potentially survivable, airplane accidents. The National Advisory Committee for Aeronautics (NACA) conducted full-scale airplane crash tests in the 1950's (refs. 1 to 3) with instrumented airplanes and later studied the dynamic response of seat structures to impact loads (ref. 4) which led to an update in static seat requirements.by the Civil Aeronautics Administration. In the 1960's, the Federal Aviation Administration (FAA) conducted transport crash tests (refs. 5 and 6), and the U.S. Army investigated Army helicopter and fixed-wing airplane accidents and identified crash injuries and injury-causing mechanisms. The Army also embarked upon a substantial crashworthiness research program which culminated in an original publication in 1967 of the Aircraft Crash Survival Design Guide. Reference 7, which is a revision of this guide, contains criteria to guide designers of Army aircraft in using special features for improving crash safety.

Since 1973, the National Aeronautics and Space Administration (NASA) and the FAA have conducted a joint study program on crash dynamics of general aviation airplanes under controlled, free-flight impact conditions. (See refs. 8 to 13.) The objective of these studies was to determine the dynamic response of airplane structures, seats,

and occupants during a crash and to determine the effect of flight parameters at impact (i.e., flight velocity, flight-path angle, pitch angle, roll angle, and ground condition) on the load and structural damage experienced by the airplane and/or occupants. During the program, 21 controlled, full-scale crash tests were performed on single-engine and twin-engine general aviation airplanes. Reference 14 provides general background information on this program. The results have provided a substantial data base on crash behavior of airplanes heretofore unavailable in the literature. Concurrently with the FAA, Civil Aeronautical Medical Institute (CAMI) has conducted an extensive, dynamic seat-test program on general aviation and U.S. Army helicopter seat designs.

The purpose of this paper is to present the results of an analysis of the crash-deceleration pulse data from the NASA/FAA crash tests to assess the effects of various flight parameters at impact on the trends of these decelerations. The analysis examined deceleration time histories resulting from vertical and longitudinal decelerations with respect to the airplane axes, effective structural crushing during the major impact phase, and the airplane slide-out distances. Data are also included from crash tests of transport airplanes. (See refs. 1, 2, and 5.) Although the airplane crash-test parameters associated with the data of this report cannot be considered comprehensive for all crash situations encountered by light airplanes, they are believed to be typical of a large percentage of crash situations. Thus, the data are believed to be of general significance regarding the assessment of expected loads at the seat/occupant structural interface for various general aviation airplanes during serious but potentially survivable crash situations.

SYMBOLS

e	horizontal distance from point of vertical (gravity axis) force to airplane center of gravity
F	force
g	acceleration due to gravity
h	vertical distance from impact surface to airplane center of gravity
I	mass moment of inertia of airplane in pitch
K	shape factor on crush distance
m	mass
s	slide-out distance
s_c	structural crush distance (normal to impact surface)
t	time
Δt	pulse duration
V	velocity of airplane
ΔV	change in velocity

X	horizontal gravity axis
X_a	longitudinal airplane axis
$\ddot{x}_a$	longitudinal deceleration in airplane X_a-axis, $\ddot{x}_a/g$, g units
$\ddot{X}_{a,max}$	maximum longitudinal deceleration, g units
$\ddot{x}$	longitudinal deceleration in X gravity axis
$\ddot{x}_a$	longitudinal deceleration in airplane X_a-axis
Z	normal (vertical) gravity axis
Z_a	vertical airplane axis
$\ddot{Z}_a$	normal (vertical) deceleration in airplane Z_a-axis, $\ddot{z}_a/g$, g units
$\ddot{Z}_{a,max}$	maximum normal deceleration, g units
$\ddot{z}$	normal deceleration in Z gravity axis
$\ddot{z}_a$	normal (vertical) deceleration in airplane Z_a-axis
γ	flight-path angle of airplane at impact
θ	pitch angle of airplane at impact
μ	coefficient of friction
$\dot{\omega}$	angular velocity
$\ddot{\omega}$	angular acceleration

Abbreviations:

c.g.	center of gravity
F.S.	fuselage station
G.A.	general aviation
WL	water line

Subscripts:

a	airplane
fp	flight path
h	horizontal
ns	normal to impact surface

p	peak
X	X-axis in gravity system
Z	Z-axis in gravity system
1	associated with major longitudinal impact
2	associated with slide-out

ANALYSIS OF CRASH SITUATION AND DISCUSSION OF RESULTS

The crash data presented in this report were derived from controlled full-scale crash tests of general aviation airplanes (refs. 8 to 13) conducted at the Langley Impact Dynamics Research Facility and from full-scale transport- and fighter-airplane tests in references 1, 2, and 5. A range of flight-path velocity, pitch angle, and flight-path angle of different airplanes impacting either a concrete or dirt surface was tested to assess the effects of these variables on the decelerations in the cabin area.

Analysis

Crash dynamics.- This section presents a discussion and analysis of a crash situation such as that shown in figures 1 and 2. Obviously, a crash is a complex occurrence with a variety of parameters contributing to the airframe loads during impact. Aerodynamic, plastic, elastic, and frictional forces interplay to remove the kinetic energy of the airplane and to change the path and alter the attitudes of the airplane. As these events occur, the seat/occupants respond to the loads and motions of the crash. Figures 1 and 3 present structural crash behavior and floor-deceleration pulses from reference 11 for a general aviation airplane and deceleration data from references 2 and 5 for transport and fighter airplanes to illustrate some of the dynamics of the complex crash scenario and to show representative deceleration pulse shapes.

The photographic sequence in figure 1(a) illustrates the crash dynamics of a single-engine, general aviation type of high-wing-airplane test specimen during a pitched-down, positive-roll (right wing down) crash starting at -0.022 sec before initial ground contact during the free-flight state after cable separation. The airplane specimen contacted the impact surface on the nose landing gear with a velocity of 25.9 m/sec along a flight-path angle of -34.5° and at a pitch angle of -39.0°, a roll angle of 18.6°, and a yaw angle of 3.2°. The nose gear started to collapse, and the engine cowling contacted the impact surface 0.028 sec after initial ground contact followed by the starboard wing tip at 0.035 sec. The windshield began to deflect and the fire wall started to penetrate the cabin at 0.060 sec. At the same time, the aft section of the fuselage began to deform and the starboard landing gear contacted the impact surface. The port landing gear contacted the impact surface at 0.130 sec into the impact, and the port wing immediately thereafter broke away from the fuselage at the aft spar and rotated forward around the front spar.

The approximate pitch attitude was retained during crash impact. At 0.15 sec, the aft cabin section pitched forward about 10° as a result of main landing-gear spring back. The airplane then settled back to about a 45° angle and continued to

skid to a stop. The fuselage cabin remained at about the same pitch, roll, and yaw angles as those of the initial impact attitude.

Time histories of the decelerations on the cabin floor are presented in figure 1(b). The normal and longitudinal decelerations extended to -20g, except for the fire wall at the floor. The fire wall contacted the impact surface and experienced -35g at about the time that the structural penetration of the cabin began. The longitudinal decelerations began at about the time that the engine cowling contacted the ground at 0.028 sec. Normal decelerations were somewhat delayed, did not start until cabin penetration had reached its maximum, and extended only over about 0.060 sec. The normal decelerations were also lower than the longitudinal deceleration, as would be expected because the airplane struck nose-on and stayed in that position during slide-out. The airplane floor decelerations were relatively low because the airplane structure absorbed much of the impact energy through structural crushing.

The shape of the pulses in figure 1(b) for both the normal and longitudinal decelerations can be approximated with a triangular shape. This approximation is used in the analysis of this paper.

A photographic sequence of a twin-engine, general aviation type of airplane crash is shown in figure 2 for a typical impact sequence of a test with $\gamma = -30°$ and $\theta = -30°$. The photographic sequences are at 0.05-sec intervals, with figure 2(b) showing conditions just prior to impact. Crushing of the nose is starting in figure 2(c). The photograph in figure 2(d) shows the engine making contact and digging into the impact surface. The initial movement of the dummy occupant, as seen through the window (but not readily visible in this sequence), occurs in figure 2(d). Shown in figure 2(e) are the wing tips lying flat on the impact surface and the cabin deformation which results in the window being broken adjacent to the first passenger and the door being opened. Figure 2(h) shows the slapdown of the aft cabin section with pronounced skin buckling behind the door. Deceleration pulse shapes similar to those representative time histories in figure 1(b) were noted also for this -30° test as well as for all the series of airplane crash tests conducted in the crash-dynamics program.

Figure 3 shows representative decelerations for a transport and a fighter airplane. (See refs. 2 and 5.) The same triangular deceleration pulse is noted in these airplane crash tests as in the general aviation airplanes; however, the duration of the pulses is generally longer as a result of the higher velocities and greater structural distances available to dissipate the impact energy in this type of airplane. Durations are basically between 0.15 and 0.3 sec as compared with 0.15 sec or less noted for the general aviation type of airplane. Compare figures 1(b) and 3 and note the data in table I.

Table I summarizes the data from the controlled crash tests of airplanes discussed in this paper. The flight-path angle, pitch angle, and flight-path velocity are given for each test number. (The nominal values of the roll and yaw angles (not included) were essentially zero with the exception of tests 9, 10, FAA-2, and FAA-3, which were tests with planned roll and/or yaw angles.) Also presented in table I are the experimental normal and longitudinal pulse data (i.e., maximum decelerations, pulse duration, velocity change, and impulse). Calculated impulse and velocity changes are included for the normal-direction pulse data.

Crash idealization.- To analyze such a complex crash scenario, a simplified situation (see sketch A) is considered and certain simplifying assumptions are made. In general, the path of the airplane will be at a flight-path angle γ to the horizontal impact surface, whereas the longitudinal (pitch) axis angle θ to the impact surface may be different from the flight path.

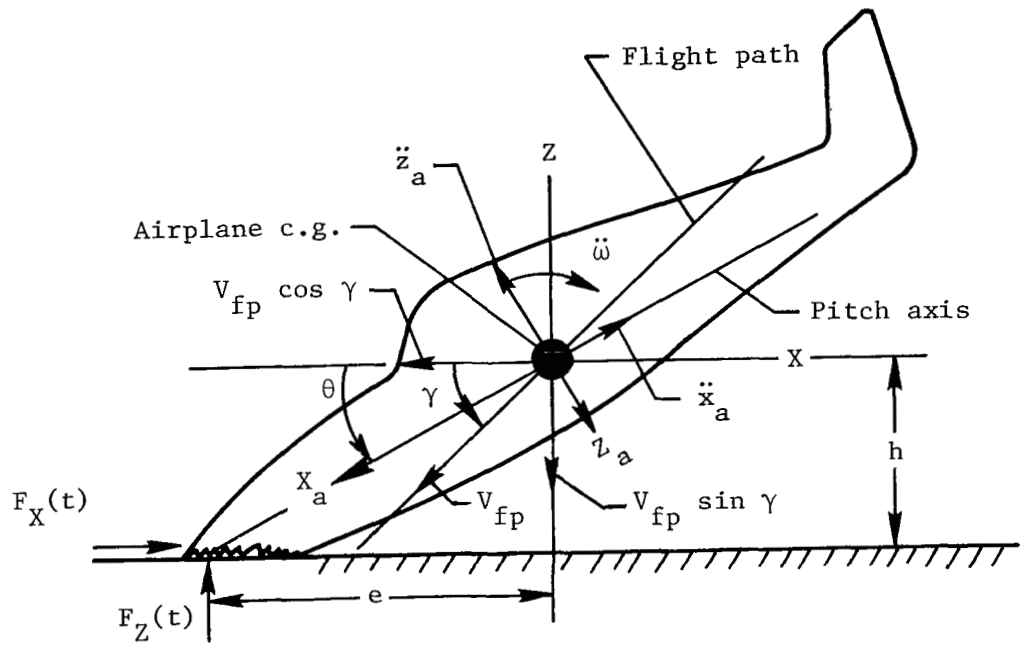

Sketch A

The airplane has a velocity V_{fp} along the flight path. The mass of the airplane is assumed to be concentrated at the c.g. (between the cockpit and cabin area on the main spar in most of the tests). Aerodynamic forces and elasticity of the structure are neglected, and yaw angles and roll angles are not considered in the present analysis. Impulsively induced rotational acceleration of the airplane is neglected during the major impact, and the airplane is assumed to be free to slide unopposed by any forces parallel to the impact surface. Assessing angular accelerations from film coverage of the controlled crash tests is very difficult, and, in actual accidents, angular accelerations are virtually impossible to estimate. The possible consequences of neglecting the angular accelerations of the airplane and assuming a frictionless situation will be discussed more fully when analytical predictions are compared with experimental data.

Equations of motion.- According to sketch A, the coupled equations of motion of the center of gravity of the airplane in the gravity axis system (X-Z plane) are

$$m\ddot{x} = F_X(t) \tag{1}$$

$$m\ddot{z} = F_Z(t) \tag{2}$$

$$I\ddot{\omega} = eF_Z(t) + hF_X(t) \tag{3}$$

Measured decelerations are in the airplane axis system (X_a-Z_a), and the transformation equations from the X-Z to the X_a-Z_a axis systems are given by

$$X_a = X \cos \theta + Z \sin \theta \tag{4}$$

$$Z_a = Z \cos \theta - X \sin \theta \tag{5}$$

The crash situation is basically an impulse problem; hence, the following approach utilizes the principle of impulse and momentum which involves force, mass, velocity, and time.

Using equations (4) and (5) and substituting into equations (1) and (2) gives

$$m\ddot{x}_a = F_X(t) \cos \theta + F_Z(t) \sin \theta \tag{6}$$

$$m\ddot{z}_a = F_Z(t) \cos \theta - F_X(t) \sin \theta \tag{7}$$

With the assumptions previously discussed, equations (6) and (7) reduce to

$$mg\ddot{X}_a = F_Z(t) \sin \theta \tag{8}$$

$$mg\ddot{Z}_a = F_Z(t) \cos \theta \tag{9}$$

where $\ddot{X}_a = \ddot{x}_a/g$ and $\ddot{Z}_a = \ddot{z}_a/g$. Since rotational accelerations are neglected, equation (3) is not essential in this computation. These equations are uncoupled equations involving the body-axis decelerations in g units, the acceleration due to gravity g, the mass of the airplane, a vertical force at the impact surface, and the pitch angle of the airplane.

Rearranging equations (8) and (9) gives, respectively,

$$F_Z(t) = \frac{mg\ddot{X}_a}{\sin \theta} \tag{10}$$

$$F_Z(t) = \frac{mg\ddot{Z}_a}{\cos \theta} \tag{11}$$

Forces Normal to Airplane Longitudinal Axis

Integration of deceleration time histories.- Based upon observations of crash-deceleration histories, the crash pulse can be approximated by a triangular deceleration (force) shape as idealized in sketch B.

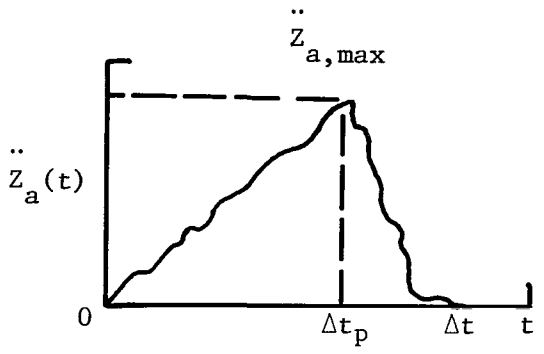

Sketch B

Using equation (11), the triangular approximation, and the principle of impulse and momentum yields

$$\int_0^{\Delta t} F_Z(t)\,dt = \frac{mg\ddot{Z}_{a,max}}{\cos\theta}\left[\int_0^{\Delta t_p} \frac{t}{\Delta t_p}\,dt + \int_{\Delta t_p}^{\Delta t} \left(\frac{\Delta t - t}{\Delta t - \Delta t_p}\right) dt\right] = m\,\Delta V_Z \qquad (12)$$

Integrating and simplifying equation (12) gives

$$\frac{mg\ddot{Z}_{a,max}}{2\cos\theta}\,\Delta t = m\,\Delta V_Z$$

and, thus,

$$\ddot{Z}_{a,max}\,\Delta t = \frac{2\,\Delta V_Z}{g}\cos\theta \qquad (13)$$

However, in sketch A the velocity change in the vertical (Z) direction, by neglecting rotation effects $\dot{\omega}$, is

$$\Delta V_{ns} = \Delta V_Z = V_{fp}\sin\gamma \qquad (14)$$

Thus,

$$\ddot{z}_{a,max}\,\Delta t = \frac{2V_{fp}}{g}\sin\gamma\cos\theta \tag{15}$$

which is the impulse on the airplane normal to the longitudinal axis in terms of the flight-path velocity, flight-path angle, pitch angle, and acceleration due to gravity.

Note that the mass of the airplane does not appear in equation (15); however, the effect of mass will be reflected in $\ddot{z}_{a,max}$ which is in nondimensional gravity units. The crash data from references 1, 2, and 8 to 13 were analyzed in terms of equation (15).

Crash impulse.- The impulse $\ddot{z}_{a,max}\,\Delta t$ is presented as a function of the change in vertical velocity ΔV_{ns} on log-log plots in figure 4. Values of the impulse computed by using the airplane attitude parameters in table I are presented in figure 4(a) as a function of the computed vertical velocity change ΔV_{ns}. The different symbols denote the various airplane types and include the data for controlled crashes of transport airplanes into dirt embankments. The linear curves presented in figure 4(a) represent analytical results for time-history approximations of triangular, half-sine, and square-wave decelerations. The experimental data are shown to be in close agreement with the triangular-deceleration crash-pulse curve.

The impulse values measured from the crash pulses of the actual test decelerations are presented in figure 4(b) as a function of the experimental velocity change ΔV_{ns}. The linear curve in the figure represents the analytical results for a triangular-deceleration pulse. Again, the measured impulse data are in good agreement with the analytical result defined by a triangular-deceleration crash-pulse shape.

To establish the validity of the assumptions which led to the uncoupled equations of motion for the crash impact, calculated impulses are plotted as a function of the experimental impulses in figure 5. The solid line in the plot represents the line of perfect agreement. The dashed line represents the least-squares curve fit passing through the plot origin. The data indicate that the calculated valves of the crash impulse (eq. (15)) are approximately 19 percent lower than the experimental values. These differences are attributed, in part, to the angular accelerations induced by the crash impact which are ignored in this simplified treatment of the problem.

Flight-path-angle effects.- The parameter $\ddot{z}_{a,max}/V_{fp}$ is presented as a function of the crash-impulse duration Δt on a log-log plot in figure 6 to illustrate the effect of flight-path angles of -15°, -30°, and -45°. The experimental crash data obtained at a flight-path angle of approximately -30° is in good agreement with analytical results. The dashed line fairing the experimental crash data obtained at a flight-path angle of about -15° indicates that the experimental data for the test conditions tend to be somewhat higher than the analytical results. This difference is again attributed, in part, to the effects of angular accelerations not included in the simplified crash model, and it appears that the effects are more pronounced for the lower flight-path angles.

Trend of Normal-Deceleration Pulse Durations

In the series of controlled crash tests, the airplanes were tested at a constant flight-path angle of -15° with the pitch angle varying from approximately 15° (nose up) to -15° (nose down).

In figure 7, the duration of the normal decelerations is plotted as a function of the pitch angle for a constant flight-path angle of -15°. Although there is scatter associated with the various decelerations in the cabin and cockpit areas, a definite trend is evident as shown by the faired curves in figure 7. The variation of pulse durations is a logical one since the shortest pulse durations occur for small pitch angles. Such crash attitudes place the minimum aircraft structure between the impact surface and the seat-structure attachments. With limited structure for crushing, short-deceleration pulses and higher peak values should be expected. For either nose-down or nose-up pitch angles along the flight path, additional aircraft structure becomes available for increasing the effective vertical crushing distance. The variation of the normal-deceleration pulse duration as a function of pitch angle is basically parabolic. For completeness of presentation, the equation of the solid faired curve in figure 7 is given as

$$\Delta t = 4.4(10^{-4})(\theta + 4)^2 + 0.052$$

Although tests were also conducted at a flight-path angle of -30°, the pitch angle for all these tests was approximately $\theta = -30°$; thus, trends for these tests cannot be evaluated. However, the available pulse-duration data are presented in table I and range from 0.05 sec up to approximately 0.15 sec. It is interesting to note and worthy of repeating that the pulse durations for the general aviation type of airplanes ranged from 0.05 to 0.15 sec, whereas the transport and fighter-type airplanes had a crash-impulse duration from 0.15 to 0.3 sec.

Structural Crush During Major Impact

Since good agreement was obtained between computed and experimental impulses on the airplane, an analytical expression for crush distance was also evaluated by using limited available data from high-speed motion-picture film of two of the crash tests.

An analytical expression for the structural crush, readily derivable for triangular pulse shapes (in terms of impact parameters), is

$$s_c = \frac{K}{\ddot{Z}_{a,max} g}(V_{fp} \sin \gamma)^2 \cos \theta \qquad (16)$$

where K, a shape factor, is equal to 1 for a symmetric triangle and to 4/3 for a ramp-type triangle.

In figure 8, s_c from equation (16) is plotted against the parameter $\frac{\ddot{z}_{a,max}}{(V_{fp} \sin \gamma)^2}$ for the NASA crash tests. As shown in the figure, the calculated values of s_c (solid symbols) lie either along or near the line for a ramp-type triangular pulse shape.

Two data points (open symbols) from film analysis are included for tests 7 and 8 and indicate that the crush of the airplane in the Z-gravity direction during the major impact can be reasonably determined by using equation (16) along with the measured $\ddot{z}_{a,max}$. Test 7, which was a very severe crash situation ($\gamma = -47.5°$, $\theta = -47.25°$), agrees better with the symmetric triangular variation; however, the results from using equation (16) give a conservative estimate of the crush distance. As a matter of interest, the crushing distance associated with the ramp-type triangular-deceleration pulse shape is larger than distances for a symmetric triangle, a half sine, a square, or an abrupt leading-edge triangular pulse shape with equal peak deceleration and velocity change.

Forces Parallel to Longitudinal Airplane Axis

In the case of the longitudinal decelerations, the overall deceleration time history has a more complex character as depicted in sketch C.

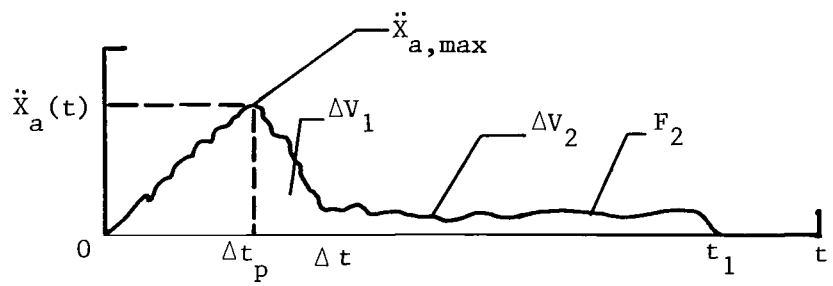

Sketch C

The longitudinal deceleration during the major impact could also be approximated as triangular (figs. 1(b) and 3); however, the velocity change ΔV must include an additional ΔV_2 which is associated with a slide-out over the impact surface.

Considering first the slide-out period between Δt and t_1 gives, from a work-kinetic energy relationship,

$$F_2 s = \frac{1}{2} m \Delta V_2^2 \tag{17}$$

where $F_2 = \mu mg$ and μ is the dynamic coefficient of sliding friction or

$$\mu mgs = \frac{1}{2} m \Delta V_2^2$$

Thus, the change in velocity during the slide-out is

$$\Delta V_2 = \sqrt{2\mu g s} \tag{18}$$

It is also known that the original component of horizontal velocity just prior to impact is (see sketch A)

$$\Delta V_{fp} \cos \gamma$$

Hence, the horizontal velocity change parallel to the impact surface prior to slide-out is

$$\Delta V_h = V_{fp} \cos \gamma - \Delta V_2$$

or

$$\Delta V_h = V_{fp} \cos \gamma - \sqrt{2g\mu s} \tag{19}$$

It is also evident that equation (19) is a component of the original ΔV along the airplane X_a-axis or

$$\Delta V_h = \Delta V_1 \cos \theta = V_{fp} \cos \gamma - \sqrt{2g\mu s} \tag{20}$$

and the velocity change parallel to the airplane X_a-axis is

$$\Delta V_1 = (V_{fp} \cos \gamma - \sqrt{2g\mu s}) \frac{1}{\cos \theta} \tag{21}$$

Using equation (10), the deceleration time-history approximation of sketch C during the major impact (0 to Δt), and impulse-momentum principles yields

$$\int_0^{\Delta t} F_Z(t) \sin \theta \, dt = mg\ddot{X}_{a,max} \left[\int_0^{\Delta t_p} \frac{t}{\Delta t_p} \, dt + \int_{\Delta t_p}^{\Delta t} \left(\frac{\Delta t - t}{\Delta t - \Delta t_p} \right) dt \right] = m \Delta V_1 \tag{22}$$

Integrating and simplifying yields

$$\frac{1}{2} mg\ddot{X}_{a,max} \Delta t = m \Delta V_1$$

or

$$\ddot{X}_{a,max} \Delta t = \frac{2}{g} \Delta V_1 \tag{23}$$

By substituting equation (21) into equation (23), the longitudinal impulse becomes

$$\ddot{X}_{a,max} \Delta t = \frac{2}{g \cos \theta}\left(V_{fp} \cos \gamma - \sqrt{2g\mu s}\right) \tag{24}$$

The longitudinal crash data from the crash-test programs were analyzed in terms of equation (24). Figure 9 presents the longitudinal impulse $\ddot{X}_{a,max} \Delta t$ plotted against the velocity change parallel to the airplane longitudinal axis, which is expressed in terms of the impact velocity and slide-out parameters. Analytical curves are shown in the figure for a triangular-deceleration pulse, a half-sine pulse, and a square pulse. Although the longitudinal-pulse data in figure 9 show somewhat greater scatter than the crash data normal to the airplane (fig. 4), the trend of the impulse is basically along the analytical curve for the triangular pulse shape with some data near the half-sine analytical curve. As was the case for the crash data normal to the airplane, the longitudinal data obtained from the transport crash tests (refs. 1 and 5) into the dirt embankments also fall on the same analytical curve as the general aviation crash-test results. Note that the agreement between the analytical and experimental longitudinal crash data involves several orders of magnitude on both the velocity change and impulse scales.

Horizontal Slide-Out Distance

As indicated in sketch C of the previous section, the horizontal slide-out distance following the major impact is a parameter of importance in assessing the longitudinal-impulse data. Slide-out distances were determined for most of the NASA data. The velocity change ΔV_2 which occurred during the slide-out are presented in figure 10 as a function of the slide-out measurements. The ΔV_2 values were determined from the known flight-path velocity and the measured ΔV_1 values during the major impact.

As shown in figure 10, the bulk of the slide-out distances lie along the line for $\mu \approx 0.42$. With the measured slide-out distances, and the velocity change during the major impact, equation (18) was used to determine the values of μ. Several low data points are the result of the airplane sliding only on the nose structure and rolling on the main gear during the slide-out period. The average value of μ of approximately 0.42 includes slide distances on concrete, asphalt, and grassy surfaces. No plowing into the surfaces occurred; thus, the data do not reflect that

aspect of a crash scenario. The crash tests with the longest slide-out distances in figure 10 were rocket-assisted crash tests at higher flight-path velocities.

Application of Results

In the previous sections, impulse data for the crash tests were determined in terms of impact parameters of the airplane prior to ground contact and for structural crush and slide-out distances after the impact. In the analysis, assumptions were made which led to uncoupled equations that gave only the product of the deceleration and time for the crash pulse. Nothing inherent in the analysis gave the magnitude or duration. However, the data can be useful in a number of applications wherein reasonable estimates can be made of the magnitude and durations of the crash pulse. Two applications are briefly outlined as follows: assessing crash-pulse data from postcrash analysis of an airplane, and assuming crash-scenario parameters from which other parameters are estimated or evaluated.

Postcrash applications.- Frequently, it is possible to obtain reasonable estimates of a number of crash parameters by examining the crash site and the airplane involved. Consider, for instance, crash 8, of which several postcrash views are shown in figure 11. An assessment of the damage pattern and crushing of that airplane indicates that this crash was most probably a nose-down impact; hence, the flight-path angle and pitch angle were probably equal in magnitude. An evaluation of the crush pattern in figure 11 transferred to figure 12, which has station reference lines, gives an estimated flight-path angle γ of -30° and pitch angle θ of -30° with an estimated structural crush distance s_c of approximately 0.95 to 1.1 m.

Accident data summarized in references 15 to 17 indicate that impact angles $\leq 30°$ and stall conditions are predominant for crashes of light, general aviation airplanes involving serious injuries. Hence, the impact velocity will be assumed to be approximately the stall velocity of this type of airplane. Thus, the estimate would be

$$V_{fp} \approx 30 \text{ m/sec}$$

Postcrash measurement of the slide-out distance from the point of impact indicated

$$s = 38 \text{ m}$$

In a crash assessment, an evaluation of the coefficient of sliding friction would be necessary along with the slide-out distance. For the majority of data of the present report, the coefficient of sliding friction was approximately 0.4. Thus, from figure 10 for a slide-out distance of 38 m, the velocity change ΔV_2 would be

$$\Delta V_2 \approx 18 \text{ m/sec}$$

Further, the velocity change during the major impact would be, by using equation (21),

$$\Delta V_1 = 9 \text{ m/sec}$$

and the vertical velocity change, by using equation (14), is

$$\Delta V_{ns} = 15 \text{ m/sec}$$

With the aforementioned data, normal and longitudinal impulses and pulse durations are calculated for both the ramp-type triangular pulse and the symmetric pulse to illustrate the shape effects on the approximations to the crash data. Thus, equation (15) gives the normal impulse

$$\ddot{Z}_{a,max} \Delta t = 2.65 \text{ sec}$$

Also, solving equation (16) for $\ddot{Z}_{a,max}$ and using an average value of 1.03 m for s_c yields

$$\ddot{Z}_{a,max} = 25.7g$$

for the ramp-type triangular shape or

$$\ddot{Z}_{a,max} = 19.3g$$

for a symmetric triangular shape. Using these results gives $\Delta t = 0.103$ sec for the ramp-type triangular-pulse duration or $\Delta t = 0.137$ sec for the symmetric triangular-shape duration.

For the longitudinal deceleration of the airplane, equation (24) gives

$$\ddot{X}_{a,max} \Delta t = 1.88 \text{ sec}$$

As a reasonable expectation, the duration of the longitudinal crash pulse is taken to be the same as the duration of the normal pulse. Hence, $\ddot{X}_{a,max} = 18.3g$ for the ramp-type triangular shape and $\ddot{X}_{a,max} = 13.7g$ for the symmetric triangular shape. A comparison of the previously given approximations of the crash results with the experimental data for this test is presented in table II.

A comparison of the calculated and experimental crash parameters in table II indicates that with reasonable after-the-fact estimates on the airplane attitude and crush distances, acceptable values can be calculated for a number of parameters of interest. Furthermore, with experimental data available from controlled crash tests as a data base, the analytical expressions presented in this paper allow the sensi-

tivity of certain parameters to variations in other parameters to be readily evaluated. This permits a reasonable range to be placed on parameters with a knowledge of how the range will affect the most important crash parameters of interest in a particular crash event.

Assumed crash scenario.- In addition to the application of the impulse data for postcrash evaluation, the data may also be utilized to evaluate a number of parameters for an assumed crash situation of interest. For example, consider the following:

An airplane impacts along a flight-path angle of $\gamma = -15°$ with a pitch angle of $\theta = 0°$. The crash situation is essentially a flat impact which places the minimum structure between the seat/occupant floor attachments and the impact surface. Stall velocity is again assumed for the flight-path velocity $V_{fp} \approx 30$ m/sec. These assumptions give

$$\gamma = -15° \qquad \theta = 0° \qquad V_{fp} \approx 30 \text{ m/sec}$$

From equation (14),

$$\Delta V_{ns} \approx 30 \sin 15° \approx 7.8 \text{ m/sec}$$

From equation (15),

$$\ddot{Z}_{a,max} \Delta t = \frac{(2)(30)(\sin 15°)(\cos 0°)}{9.8} \approx 1.6 \text{ sec}$$

and $\ddot{Z}_{a,max}$, from equation (16), then gives

$$\ddot{Z}_{a,max} = \frac{4}{3s_c(9.8)}[30(\sin 15°)]^2 \cos 0°$$

$$\ddot{Z}_{a,max} = \frac{8.203}{s_c}$$

Calculations of $\ddot{Z}_{a,max}$ for various assumed crush distances can be made; or, conversely, for assumed or desirable $\ddot{Z}_{a,max}$, the required, effective, structural crush distance s_c can be evaluated. For the sake of illustration, assume 0.3 m of crushing (lower end of crushing for approximately seven crash tests shown in fig. 10). Thus,

$$s_c \approx 0.3 \text{ m}$$

Then, from the previous equations,

$$\ddot{z}_{a,max} = \frac{8.203}{0.3} = 27.3g$$

and

$$\Delta t = \frac{1.6}{27} \approx 0.059 \text{ sec}$$

A number of variations using the aforementioned approach can be examined to assess the influence of the various parameters on the expected decelerations, times, and crush distances. For the longitudinal decelerations of the scenario, equation (24) gives

$$\ddot{x}_{a,max} \Delta t = 0.204(28.98 - 2.8\sqrt{s})$$

where $\mu = 0.4$ has been assumed. With the given conditions, the effects of various velocity changes or the slide-out distance s following the major impact can be determined. The limitation on the slide-out distance s would have to be

$$s \leq \frac{(28.98)^2}{(2.8)^2} \leq 107 \text{ m}$$

which would imply essentially no velocity change during the major impact. A number of the controlled crash tests indicated velocity changes ΔV_1 between 4 to 10 m/sec during the major impact. If similar velocity changes are assumed for this example, the result would be

$$\ddot{x}_{a,max} \Delta t = 0.204 \Delta V_1$$

$$= 0.82 \text{ sec} \qquad (\Delta V_1 = 4 \text{ m/sec})$$

$$= 2.04 \text{ sec} \qquad (\Delta V_1 = 10 \text{ m/sec})$$

By using the pulse duration associated with the vertical-deceleration pulse, the decelerations would be, for the velocity change of 4 m/sec,

$$\ddot{X}_{a,max} = \frac{0.82}{0.059} = 13.9g$$

or, for the velocity change of 10 m/sec,

$$\ddot{X}_{a,max} = \frac{2.04}{0.059} = 34.6g$$

The corresponding slide-out distances would be

$$s = \left(\frac{28.98 - \Delta V_1}{2.8}\right)^2$$

where, for the velocity change of 4 m/sec,

$$s = \left(\frac{28.98 - 4}{2.8}\right)^2 = 79.6 \text{ m}$$

and, for the velocity change of 10 m/sec,

$$s = \left(\frac{28.98 - 10}{2.8}\right)^2 = 45.9 \text{ m}$$

With knowledge of expected deceleration magnitudes for various effective crush distances, slide-out distances, and velocity changes, a designer would have the basis for altering the strength of fuselage subfloors to lower the force level during collapse, for designing seats to incorporate load-limiting features, and for evaluating other aspects of design for a goal for a particular upper-limit crash-design scenario. Obviously, there are limits to what can be done to extend the range of critical crash parameters to encompass as many crash situations as possible while improving crash survivability. However, with simplified analyses which provide reasonable estimates of crash parameters and with a data base of experimental information with which to compare, design changes could begin to find their way into a new generation of airplanes which hopefully could improve the crash survivability of occupants.

CONCLUDING REMARKS

An analysis has been made of crash-deceleration pulse data from a crash-dynamics program on general aviation airplanes and from previously published transport crash data available in the literature. This crash-dynamics program has been a joint

effort since 1973 by the National Aeronautics and Space Administration (NASA) and the Federal Aviation Administration (FAA). The purpose of the analysis was to correlate and assess structural airplane crash data with flight parameters at impact.

In the analysis, assumptions made to simplify the complex crash scenario led to uncoupled equations for the normal and longitudinal impulses in the cabin area of the airplane. Analytical expressions, structural crush distances, and slide-out were also determined. Good agreement was found between experimental and analytical data for the general aviation and transport airplanes over a wide range of impact parameters.

Applications of the analysis were presented for postcrash evaluation of crash parameters and an assumed crash scenario. Although the values of airplane crash-test parameters associated with the data of this report cannot be considered comprehensive for all crash situations encountered by light airplanes, they are believed to be typical of a large percentage of crash situations. Thus, the information in this report is believed significant to assess loads at the seat/occupant structure interface for general aviation airplanes during serious but potentially survivable crashes.

Langley Research Center
National Aeronautics and Space Administration
Hampton, VA 23665
September 20, 1982

REFERENCES

1. Preston, G. Merritt; and Pesman, Gerard J.: Accelerations in Transport-Airplane Crashes. NACA TN 4158, 1958.

2. Acker, Loren W.; Black, Dugald O.; and Moser, Jacob C.: Acceleration in Fighter-Airplane Crashes. NACA RM E57G11, 1957.

3. Eiband, A. Martin; Simpkinson, Scott H.; and Black, Dugald O.: Accelerations and Passenger Harness Loads Measured in Full-Scale Light-Airplane Crashes. NACA TN 2991, 1953.

4. Pinkel, I. Irving; and Rosenberg, Edmund G.: Seat Design for Crash Worthiness. NACA Rep. 1332, 1957.

5. Reed, W. H.; Robertson, S. H.; Weinberg, L. W. T.; and Tyndall, L. H.: Full-Scale Dynamic Crash Test of a Lockheed Constellation Model 1649 Aircraft. FAA-ADS-38, Oct. 1965.

6. Reed, W. H.; Robertson, S. H.; Weinberg, L. W. T.; and Tyndall, L. H.: Full-Scale Dynamic Crash Test of a Douglas DC-7 Aircraft. FAA-ADS-37, Apr. 1965.

7. Aircraft Crash Survival Design Guide. U.S. Army.
   Desjardins, S. P.; and Laananen, D. H.; and Singley, G. T., III: Volume I - Design Criteria and Checklists. USARTL-TR-79-22A, Dec. 1980. (Available from DTIC as AD A093 784.)
   Laananen, D. H.: Volume II - Aircraft Crash Environment and Human Tolerance. USARTL-TR-79-22B, Jan. 1980. (Available from DTIC as AD A082 512.)
   Laananen, D. H.; Singley, G. T., III; Tanner, A. E.; and Turnbow, J. W.: Volume III - Aircraft Structural Crash-Worthiness. USARTL-TR-79-22C, Aug. 1980. (Available from DTIC as AD A089 104.)
   Desjardins, S. P.; and Laananen, D. H.: Volume IV - Aircraft Seats, Restraints, Litters, and Padding. USARTL-TR-79-22D, June 1980. (Available from DTIC as AD A088 441.)
   Johnson, N. B.; and Robertson, S. H.: Volume V - Aircraft Postcrash Survival. USARTL-TR-79-22E, Jan. 1980. (Available from DTIC as AD A082 513.)

8. Alfaro-Bou, Emilio; and Vaughan, Victor L., Jr.: Light Airplane Crash Tests at Impact Velocities of 13 and 27 m/sec. NASA TP-1042, 1977.

9. Castle, Claude B.; and Alfaro-Bou, Emilio: Light Airplane Crash Tests at Three Flight-Path Angles. NASA TP-1210, 1978.

10. Castle, Claude B.; and Alfaro-Bou, Emilio: Light Airplane Crash Tests at Three Roll Angles. NASA TP-1477, 1979.

11. Vaughan, Victor L., Jr.; and Hayduk, Robert J.: Crash Tests of Four Identical High-Wing Single-Engine Airplanes. NASA TP-1699, 1980.

12. Vaughan, Victor L., Jr.; and Alfaro-Bou, Emilio: Light Airplane Crash Tests at Three Pitch Angles. NASA TP-1481, 1979.

13. Alfaro-Bou, Emilio; Williams, M. Susan; and Fasanella, Edwin L.: Determination of Crash Test Pulses and Their Application to Aircraft Seat Analysis. SAE Tech. Paper 810611, Apr. 1981.

14. Hayduk, Robert J.; Thomson, Robert G.; and Carden, Huey D.: NASA/FAA General Aviation Crash Dynamics Program - An Update. Forum, vol. 12, no. 3, Winter 1979, pp. 147-156.

15. Wittlin, Gil: Development, Experimental Verification and Application of Program 'KRASH' for General Aviation Airplane Structural Crash Dynamics, FAA-RD-78-119, Dec. 1978.

16. Wittlin, Gil; Gamon, Max A.; and LaBarge, William L.: Full Scale Crash Test Experimental Verification of a Method of Analysis for General Aviation Airplane Structural Crashworthiness. Rep. No. FAA-RD-77-188, Feb. 1978. (Available from DTIC as AD A054 154.)

17. Vaughan, Victor L., Jr.; and Alfaro-Bou, Emilio: Impact Dynamics Research Facility for Full-Scale Aircraft Crash Testing. NASA TN D-8179, 1976.

TABLE I.- SUMMARY OF DATA FROM CONTROLLED CRASH TESTS OF AIRPLANES

(a) Experimental and calculated normal pulse parameters

Test	Flight-path angle, γ, deg	Pitch angle, θ, deg	Flight-path velocity, V_{fp}, m/sec	Experimental normal pulse parameters				Calculated normal pulse parameters	
				Maximum deceleration, $\ddot{z}_{a,max}$, g units	Pulse duration, Δt, sec	Velocity change, ΔV_z, m/sec	Impulse, $\ddot{z}_{a,max}\ \Delta t$, sec	Impulse, $\ddot{z}_{a,max}\ \Delta t$, sec	Velocity change, ΔV_z, m/sec
2	-16	-12	27	20	0.089	8.5	1.78	1.49	7.44
3	-18.75	-18	26.2	28	.05	8.74	1.40	1.63	8.42
4	-15	4	27	16	.102	8.5	1.63	1.42	6.99
5	-20.5	-19.5	26.1					1.76	9.14
6	-16	14	27	18	.110	10.4	1.98	1.47	7.44
7	-47.5	-47.25	28.6	20	0.174	20.73	3.48	2.92	21.1
8	-30	-31	27	18	.135	13	2.43	2.36	13.5
9	-16	-13	26.3					1.44	7.25
10	-18	-14	27.8					1.70	8.59
11	-31	-27	25	12	.132	10	1.58	2.34	12.87
12	-15	9	25	12	0.149	9.5	1.79	1.30	6.47
13	-29	-26	25	27	.049	13	1.32	2.22	12.12
14	-16.75	-11.75	32.7					1.88	9.42
15	-18	-12	41	46	.064	17	2.94	2.53	12.67
16	-15	-4	40	46	.054	15	2.48	2.11	10.35
17	-30	-38	40	42	0.097	19	4.07	3.22	20.0
18	-30	-31	27.9	27.2	.083	11.3	2.26	2.34	13.5
19	-15	-17.7	27	16	.12	10.6	1.92	1.38	6.99
20	-15.4	2	26.6	31	.057	9.1	1.77	1.43	6.99
21	-30	-29.5	27.1	29.9	.096	12.3	2.87	2.39	13.5
FAA-1	-32	-30	25	21	0.120	11	2.52	2.34	13.24
FAA-2	-17	-13.5	23	7	.160	6	1.12	1.33	6.72
FAA-3	-34.5	-39	25.9	18	.12	13.8	2.2	2.33	14.7
FAA-4	-32	-34.5	25.3	18	.13	14.8	2.34	2.25	13.41
				(a) (b)	(a) (b)	(a) (b)	(a) (b)		
Fighter (ref. 2)	-18	-18	50					3.0	15.45
	-22	-22	50	30	0.142	23	4.26	3.54	18.73
	-27	-27	50	37.5 22	.13 0.21	21.6 22	4.88 4.62	4.13	22.7
Transport (ref. 1)	-14	-14	48.7	11.4	0.25	12	2.85	2.33	11.8
	-27	-27	48.7	23.3	.21	21	4.89	4.02	22.1
Transport (ref. 5):									
F.S. 1165	-6	-6	57.7						
F.S. 685 c.g.				7	0.26	9.4	1.82	1.22	6
Cub type (ref. 3)	-55	-55	26.8						
	-55	-55	21						
	-55	-55	18.8						

[a]Values in the cockpit.
[b]Values at the c.g.

TABLE I.- Concluded

(b) Experimental longitudinal pulse parameters

Test	Flight-path angle, γ, deg	Pitch angle, θ, deg	Experimental longitudinal pulse parameters							
			Flight-path velocity, V_{fp}, m/sec	Maximum deceleration, $\ddot{x}_{a,max}$, g units		Pulse duration, Δt, sec		Velocity change, ΔV_1, m/sec		Impulse $\ddot{x}_{a,max}\ \Delta t$, sec	
2	-16	-12	27	19		0.06		6		1.14	
3	-18.75	-18	26.2	18		.044		4.3		.79	
4	-15	4	27	7		.101		5		.71	
5	-20.5	-19.5	26.1								
6	-16	14	27	8		.110		3.1		.86	
7	-47.5	-47.25	28.6	8.8		0.144		[a]4.6; 6.8; 9		1.27	
8	-30	-31	27	16		.110		6		1.76	
9	-16	-13	26.3								
10	-18	-14	27.8								
11	-31	-27	25	28		.138		17.7		3.86	
12	-15	9	25	4		0.060		1.2		0.24	
13	-29	-26	25	11		.093		5		1.02	
14	-16.75	-11.75	32.7								
15	-18	-12	41	16		.058		5		.93	
16	-15	-4	40	12		.062		4		.744	
17	-30	-38	40	22		0.068		10		1.5	
18	-30	-31	27.9	15.2		.090		8.2		1.37	
19	-15	-17.7	27	5.5		.088		4		.48	
20	-15.4	2	26.6	6.4		.052		1.9		.333	
21	-30	-29.5	27.1	14		.112		10.5		1.57	
FAA-1	-32	-30	25	22		0.110		8		2.42	
FAA-2	-17	-13.5	23	3.5		.060		1.5		.21	
FAA-3	-34.5	-39	25.9	17		.13		12		2.21	
FAA-4	-32	-34.5	25.3	45		.10		21.5		4.5	
				(b)	(c)	(b)	(c)	(b)	(c)	(b)	(c)
Fighter (ref. 2)	-18	-18	50	23	16.8	0.10	0.23	12	19.5	2.3	3.81
	-22	-22	50	25	23.3	.18	.21	22	24	4.5	4.92
	-27	-27	50	40	50	.13	.22	26	45	5.2	11.1
Transport (ref. 1)	-14	-14	48.7	7.1		0.21		7.6		1.5	
	-6	-6	57.7	19.2		.36		29.3		6.9	
Transport (ref. 5):											
F.S. 1165				8		0.235		9.5		1.88	
F.S. 923				8.4		.23		9.5		1.93	
F.S. 685 c.g.				9.0		.23		9.5		2.07	
F.S. 460 c.g.				9.6		.24		9.5		2.3	
F.S. 195 c.g.				11.4		.14		9.5		1.6	
Cub type (ref. 3)	-55	-55	26.8	25.2		0.19		27		4.92	
	-55	-55	21	22		.224		21		4.93	
	-55	-55	18.8	18.4		.24		18.8		4.42	

[a]The value 4.6 indicates slide-out (see eq. (21)); 6.8 denotes the average of film and slide-out analysis; and 9 is taken from film analysis.

[b]Values in the cockpit.

[c]Values at the c.g.

TABLE II.- COMPARISON OF EXPERIMENTAL AND ESTIMATED CRASH PARAMETERS

Parameter	Experimental	Estimated (computed)
γ, deg	-30	-30
θ, deg	-31	-30
V_{fp}, m/sec	27	30
ΔV_1, m/sec	6	9
ΔV_{ns}, m/sec	13	15
s, m	38	
s_c, m	1.17 (film)	0.95 to 1.1 (1.03 av.)
$\ddot{Z}_{a,max}$ Δt, sec	2.43	2.65
$\ddot{Z}_{a,max}$, g units	18.0	19.3 26.0
Δt, sec	0.135	0.103 to 0.137
$\ddot{X}_{a,max}$ Δt, sec	1.76	1.88
$\ddot{X}_{a,max}$, g units	16.0	13.7 18.3
Δt, sec	0.11	0.10 to 0.137

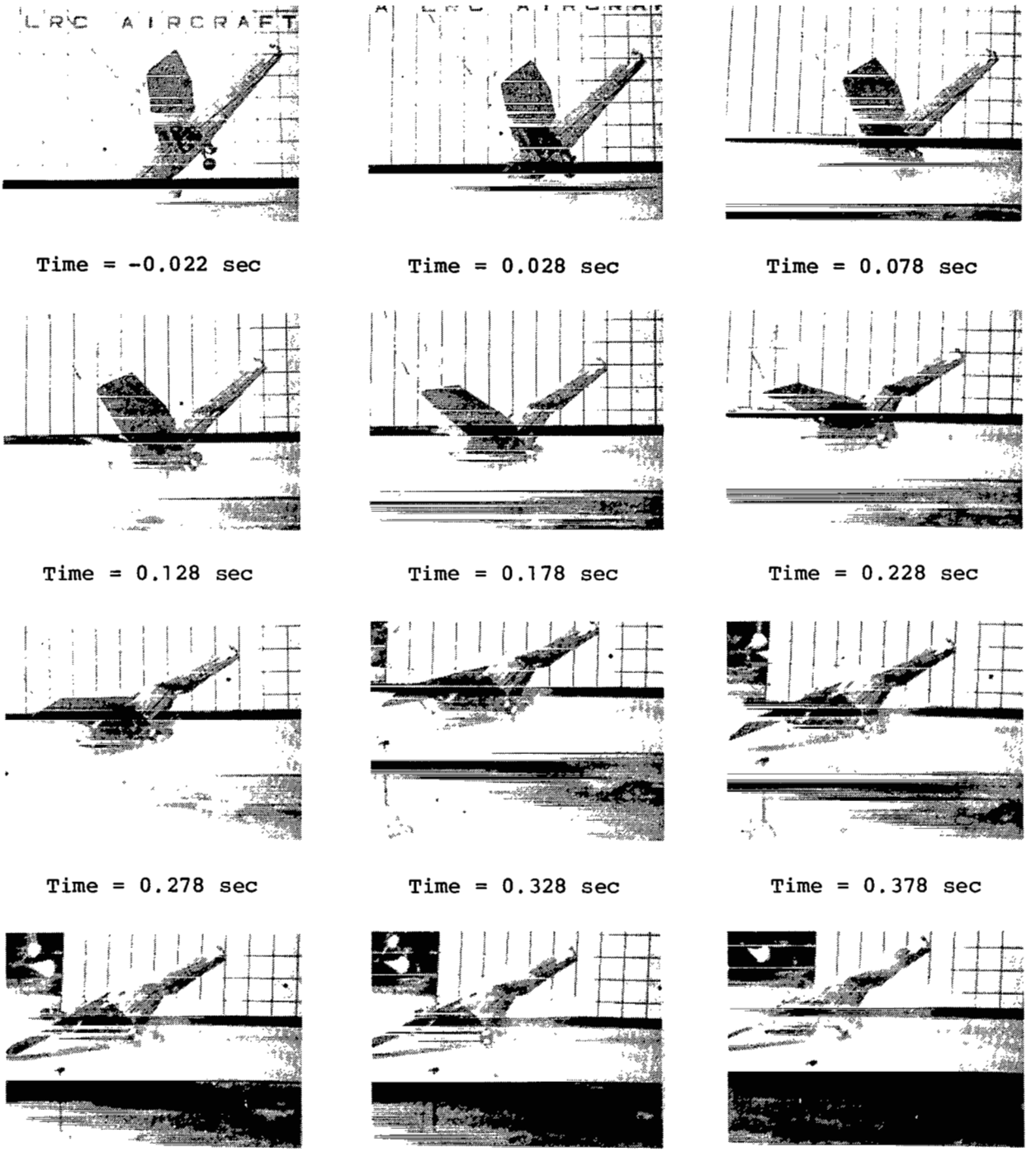

(a) Crash dynamics.

Figure 1.- Crash-test results of a high-wing, single-engine airplane.

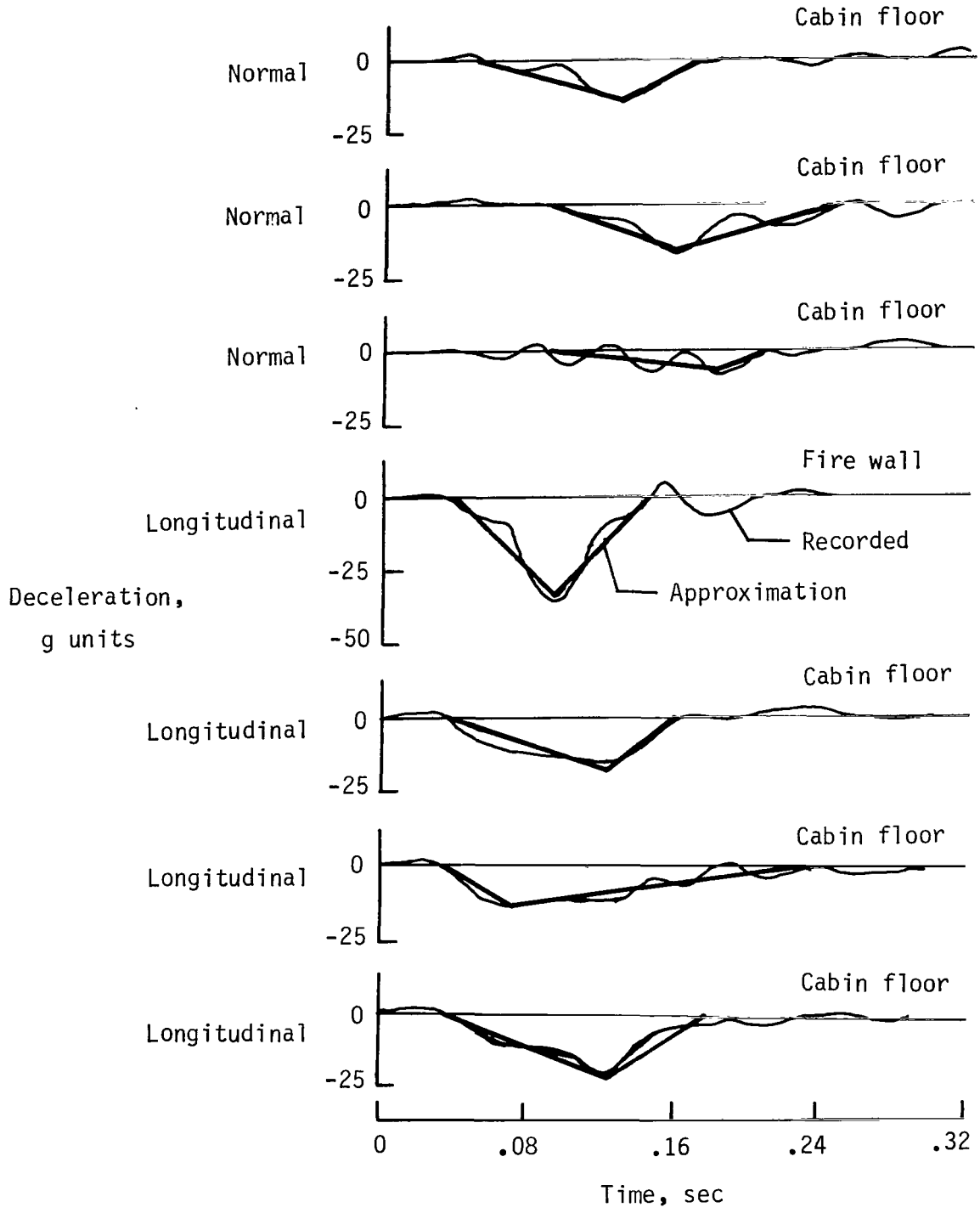

(b) Decelerations.

Figure 1.- Concluded.

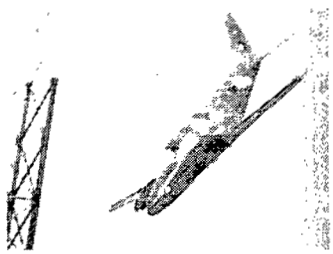

(a) Prior to impact.

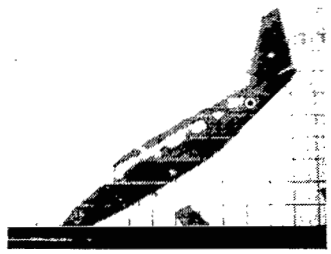

(b) Time = -0.01 sec.

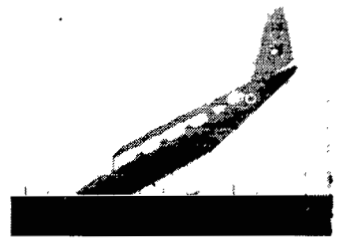

(c) Time = 0.04 sec.

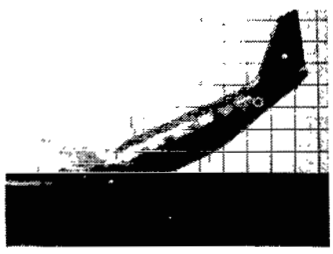

(d) Time = 0.09 sec.

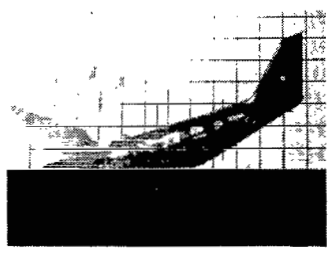

(e) Time = 0.14 sec.

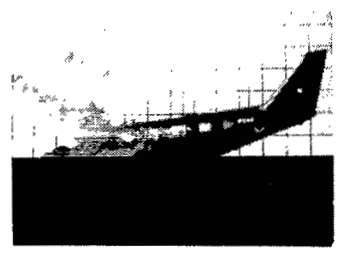

(f) Time = 0.19 sec.

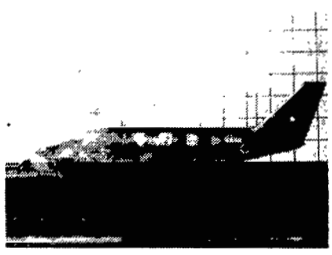

(g) Time = 0.24 sec.

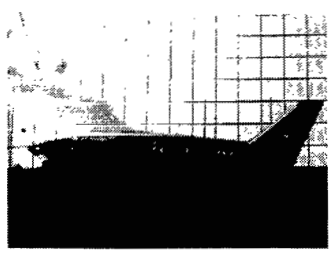

(h) Time = 0.29 sec.

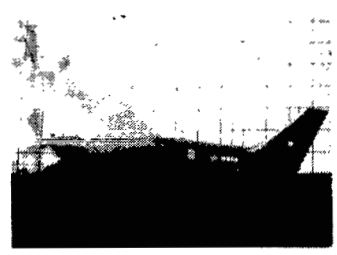

(i) Time = 0.34 sec.

(j) Time = 0.39 sec.

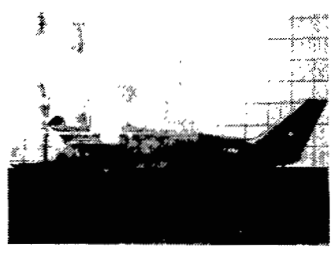

(k) Time = 0.44 sec.

(l) Time = 0.49 sec.

L-78-97

Figure 2.- Photographic sequence of a crash test of a twin-engine airplane.

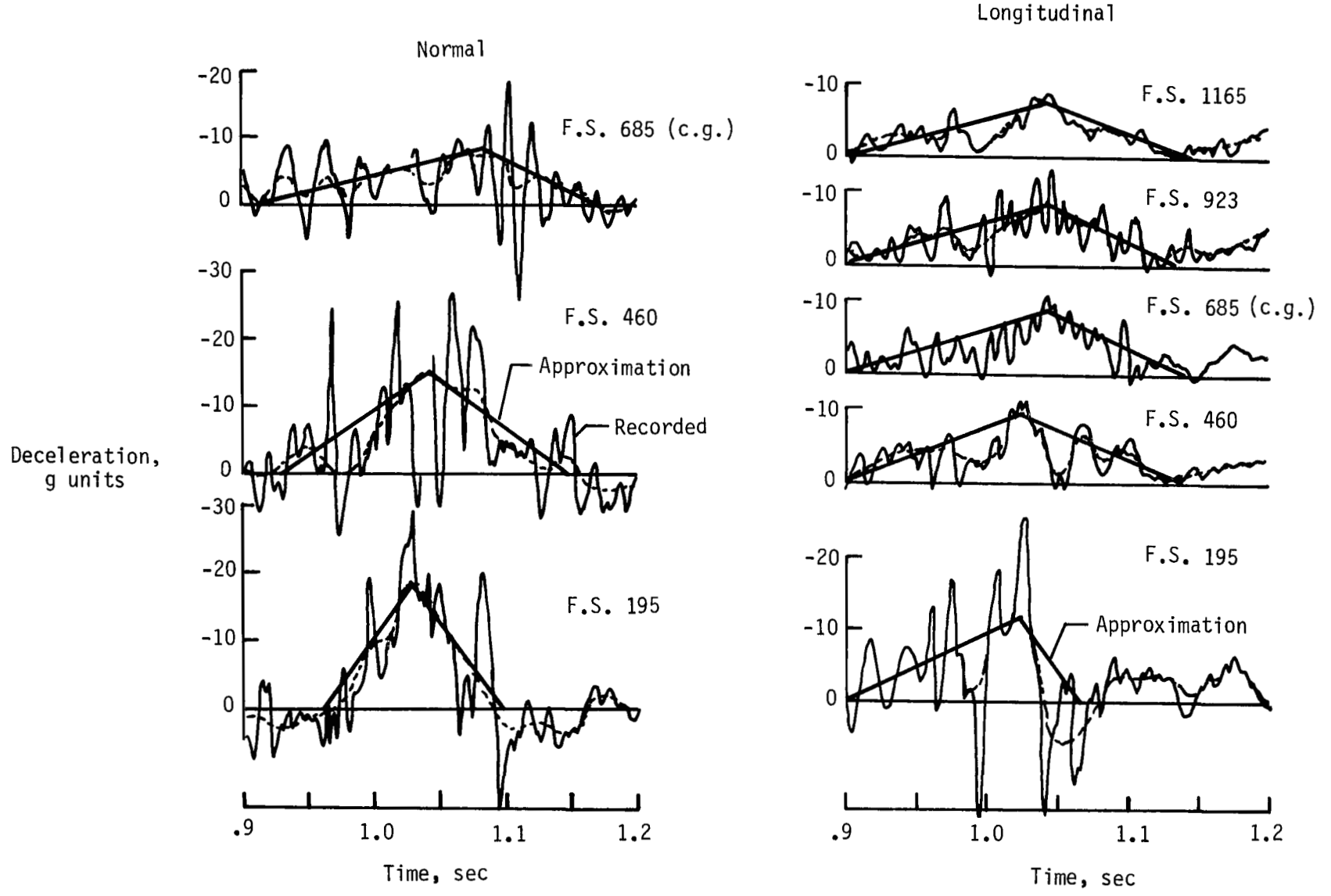

(a) Transport airplane.

Figure 3.- Typical time histories for normal and longitudinal decelerations.

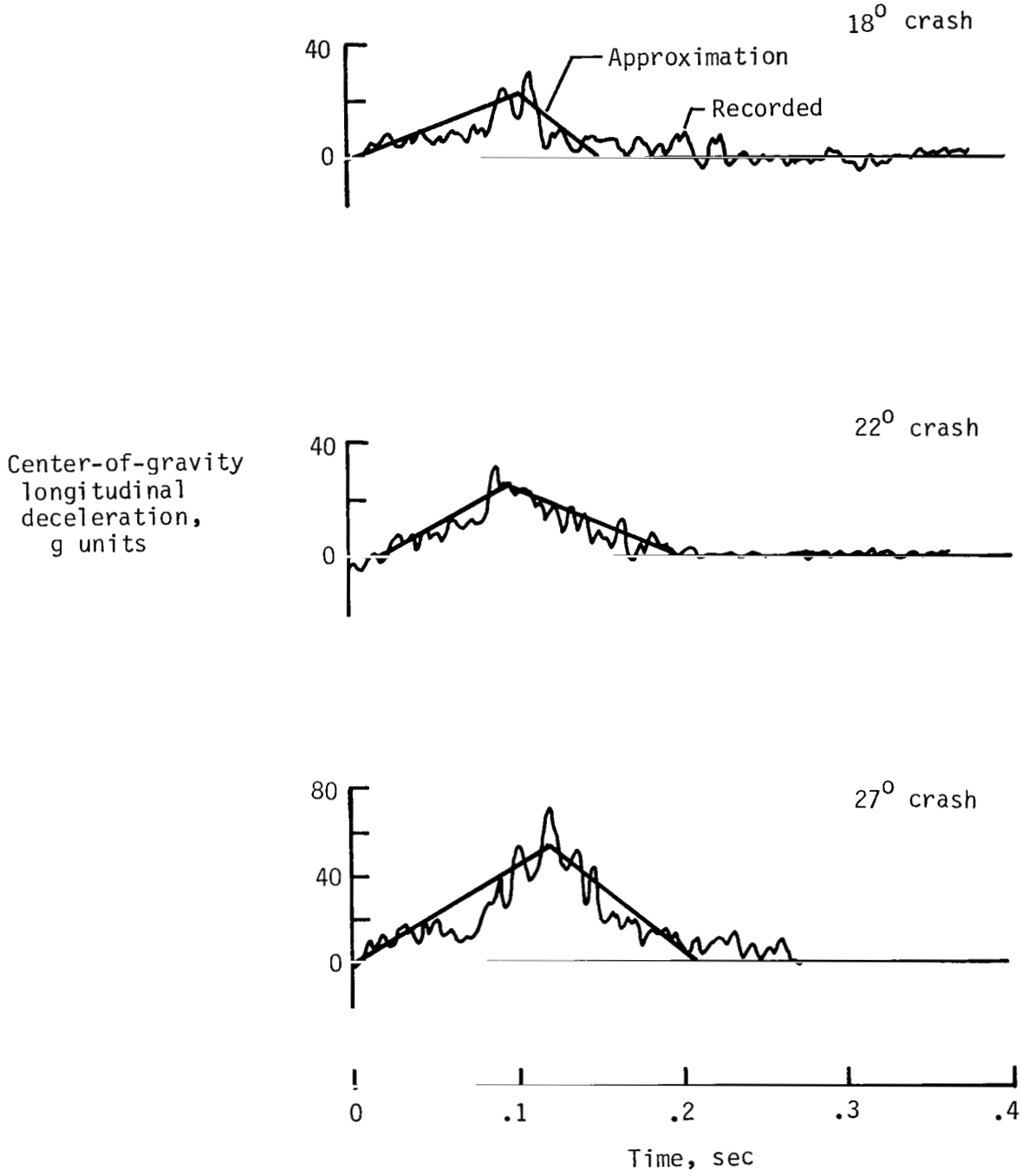

(b) Fighter airplane.

Figure 3.- Concluded.

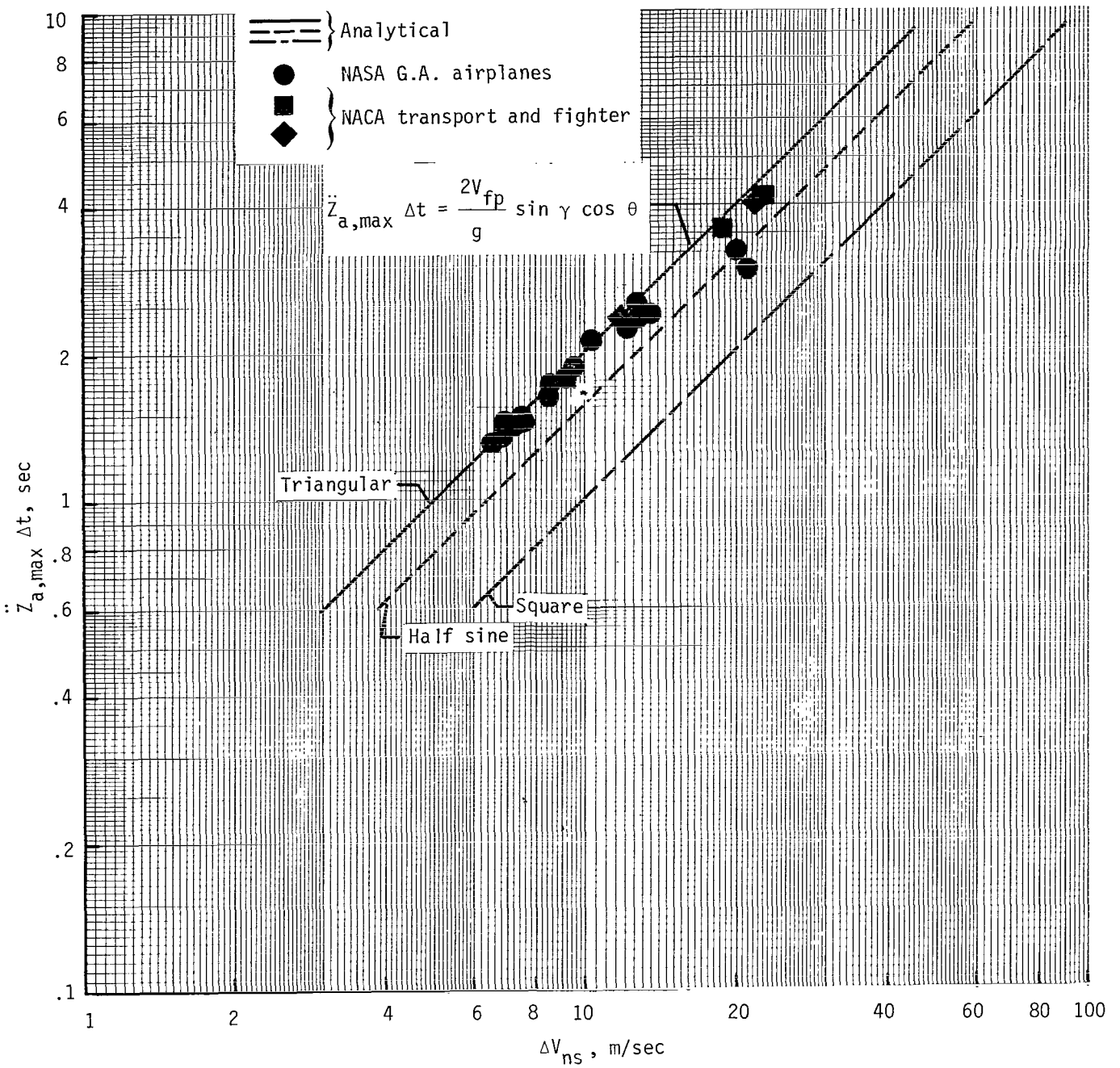

(a) Calculated normal impulse.

Figure 4.- Experimental and calculated normal-impulse data for airplane crashes.

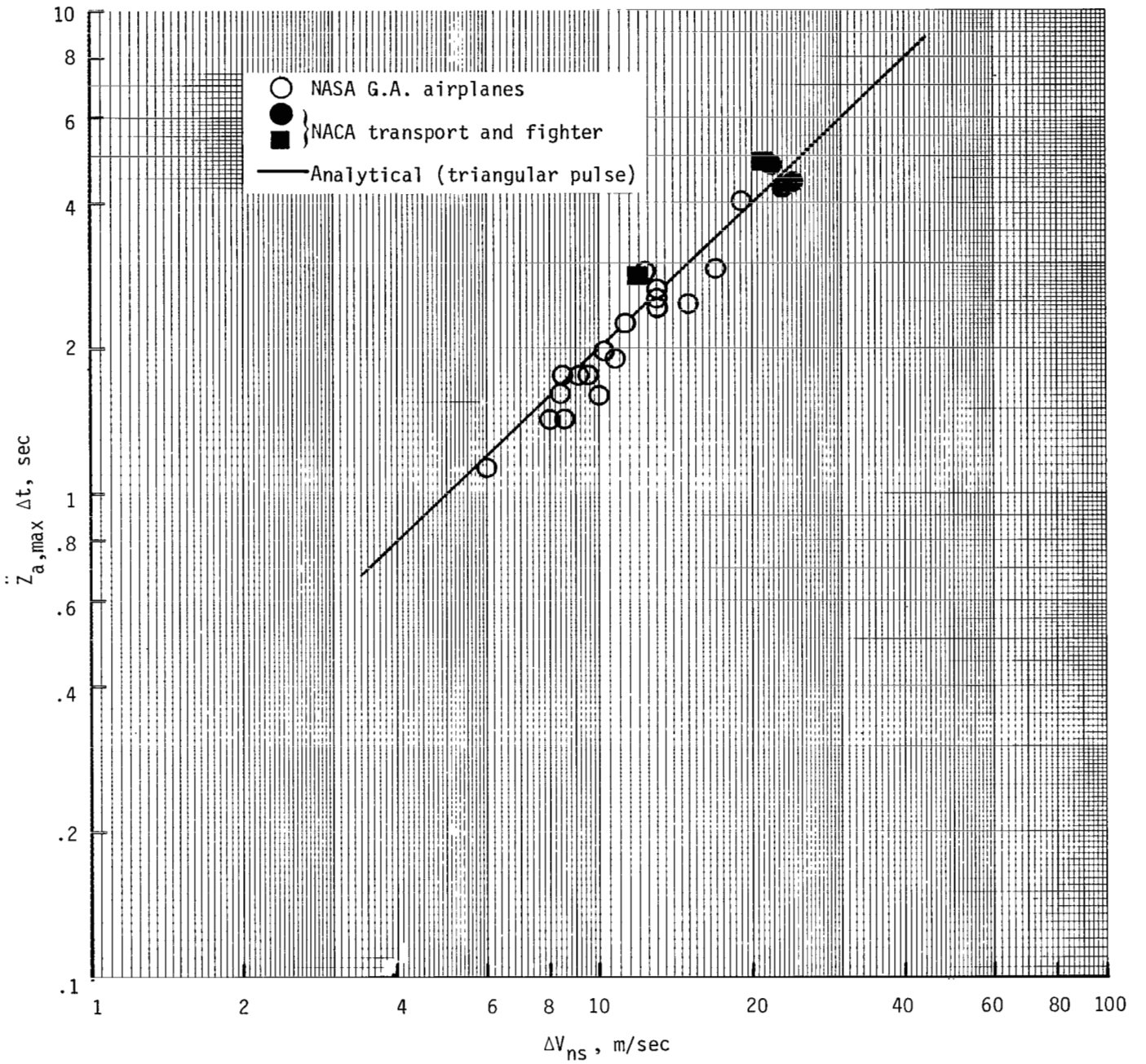

(b) Experimental normal impulse.

Figure 4.- Concluded.

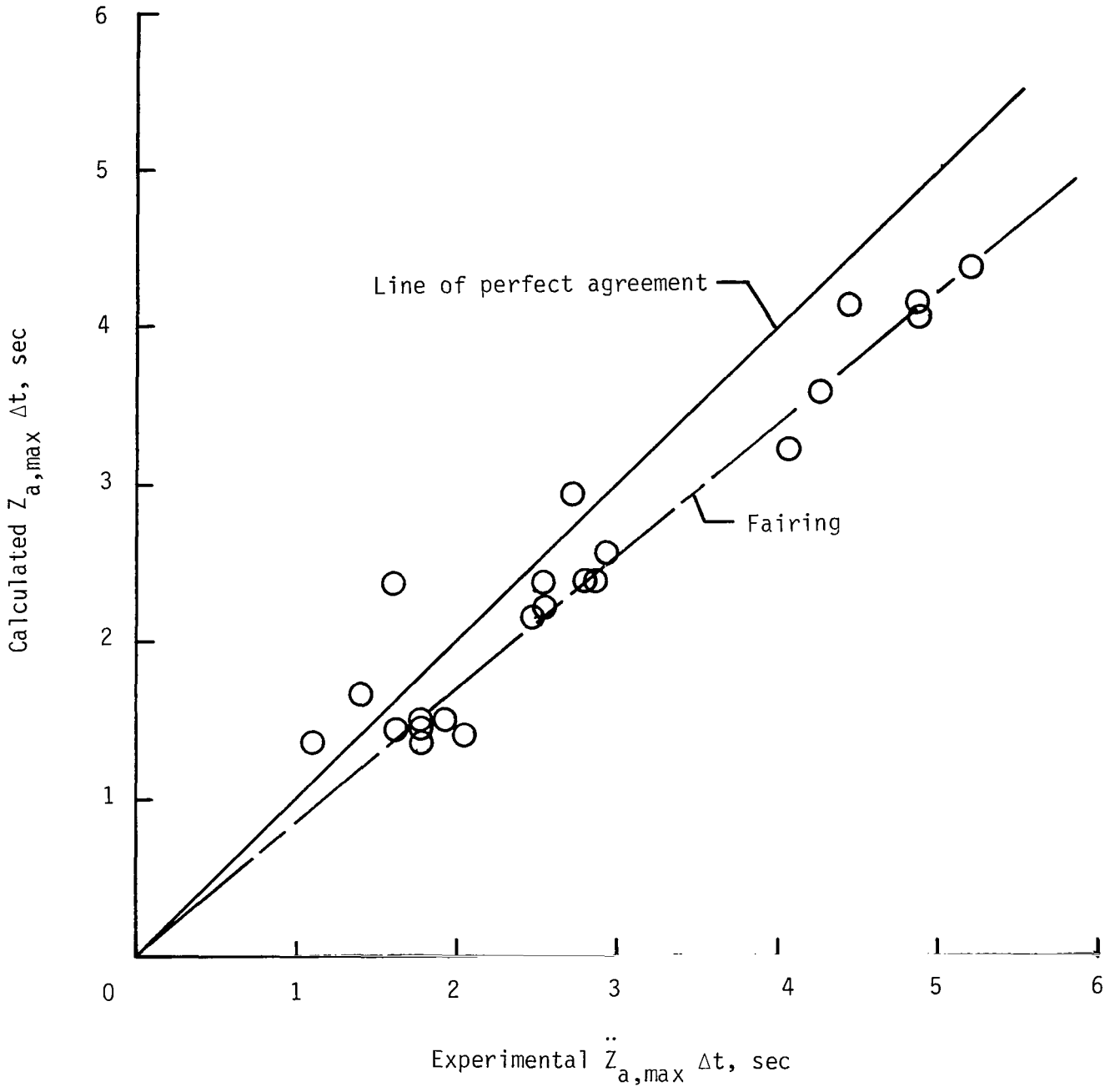

Figure 5.- Calculated normal pulse plotted against experimental normal impulse.

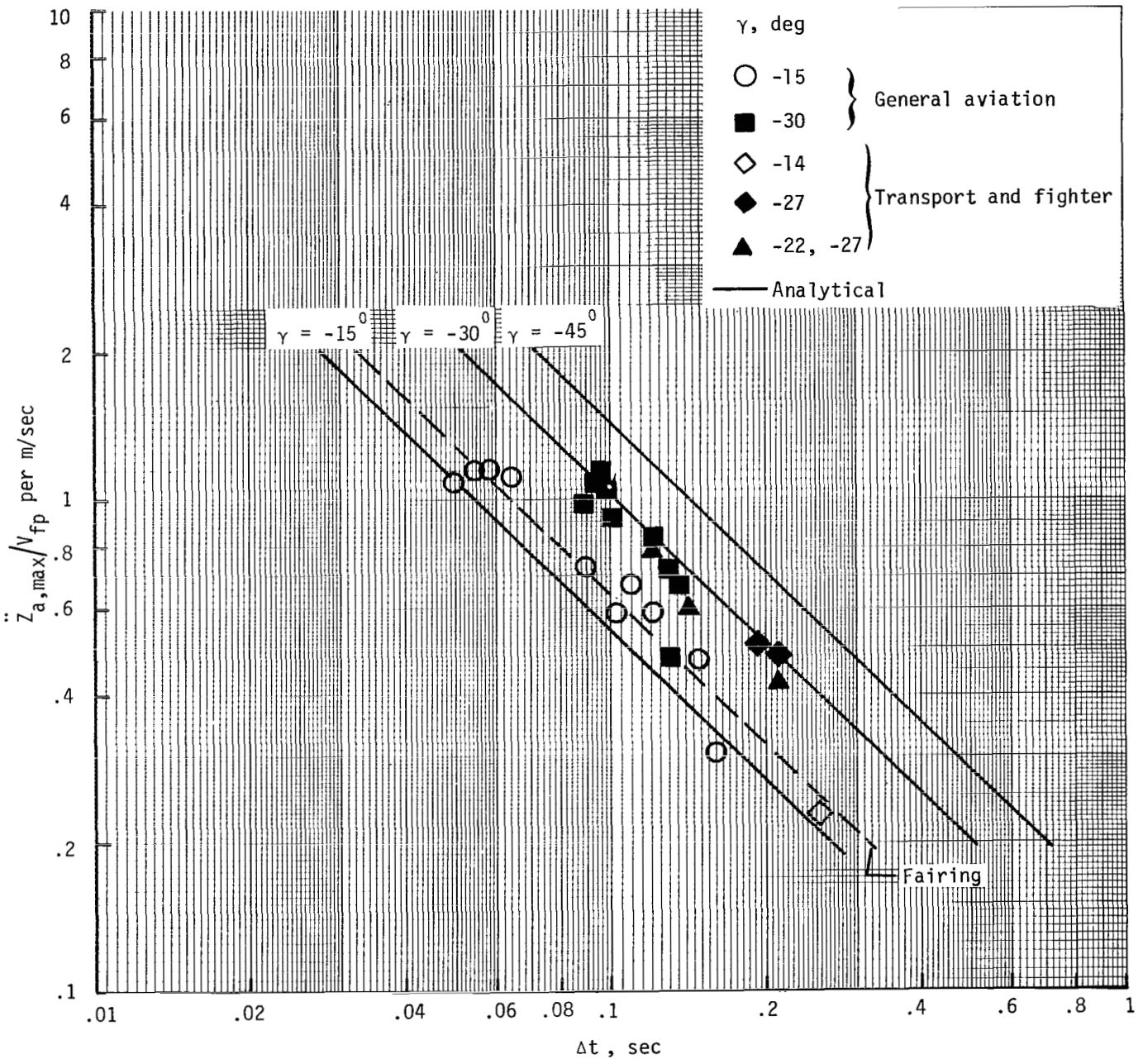

Figure 6.- Effect of flight-path angle on normal impulses.

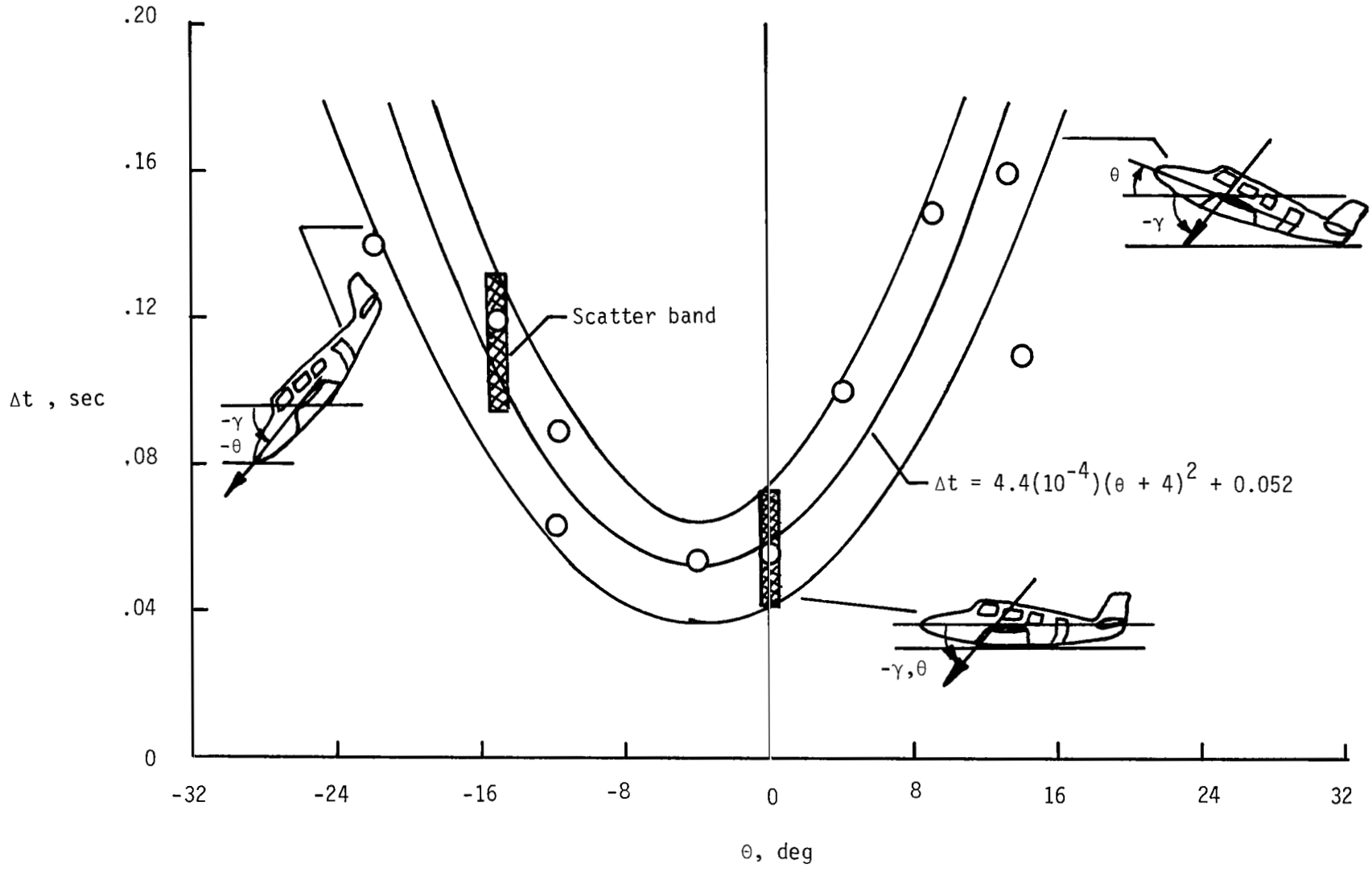

Figure 7.- Normal-deceleration pulse duration plotted against pitch angle.
$\gamma = -15°$; $V_{fp} \approx$ Constant.

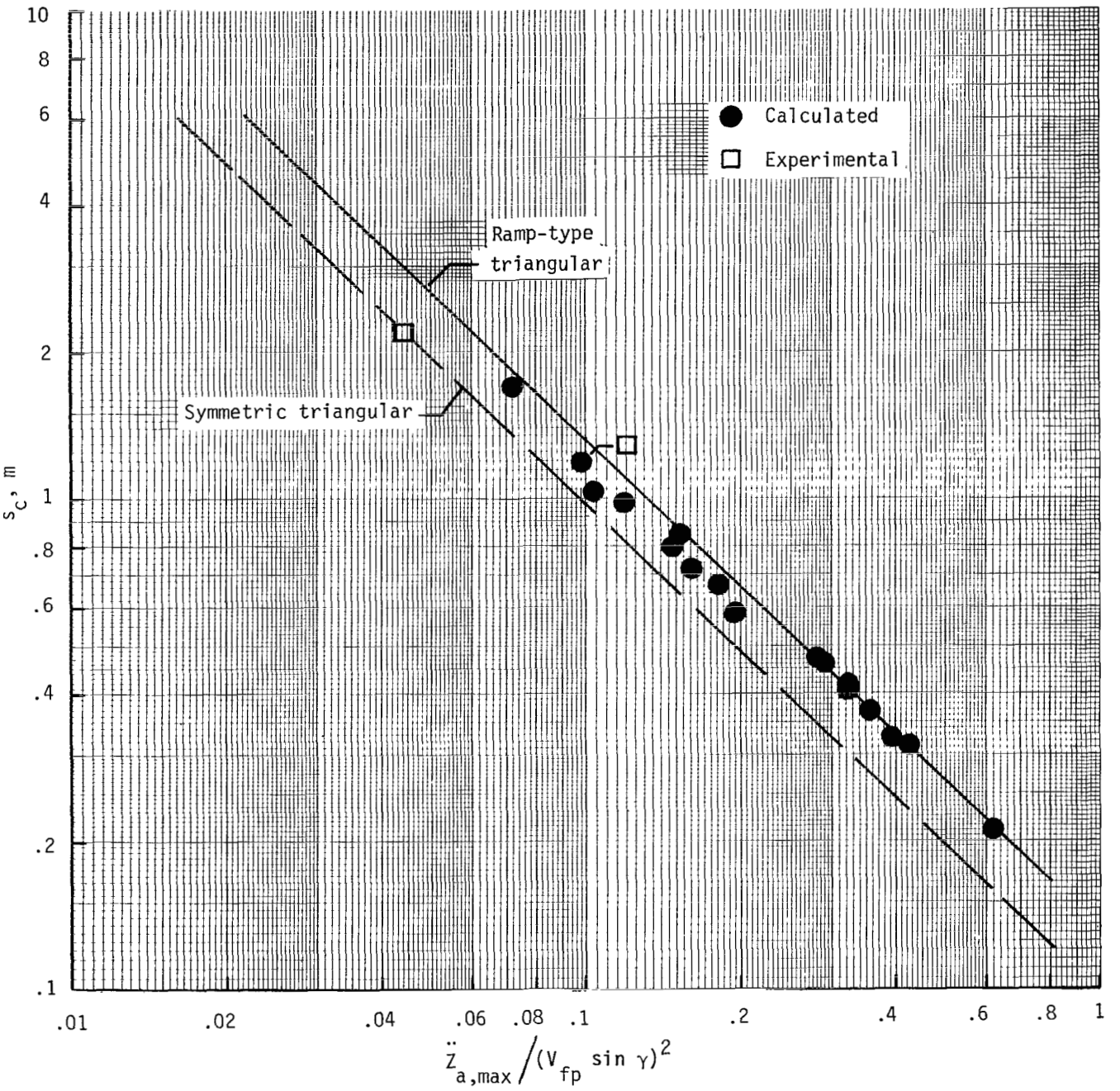

Figure 8.- Structural crush normal to impact surface.

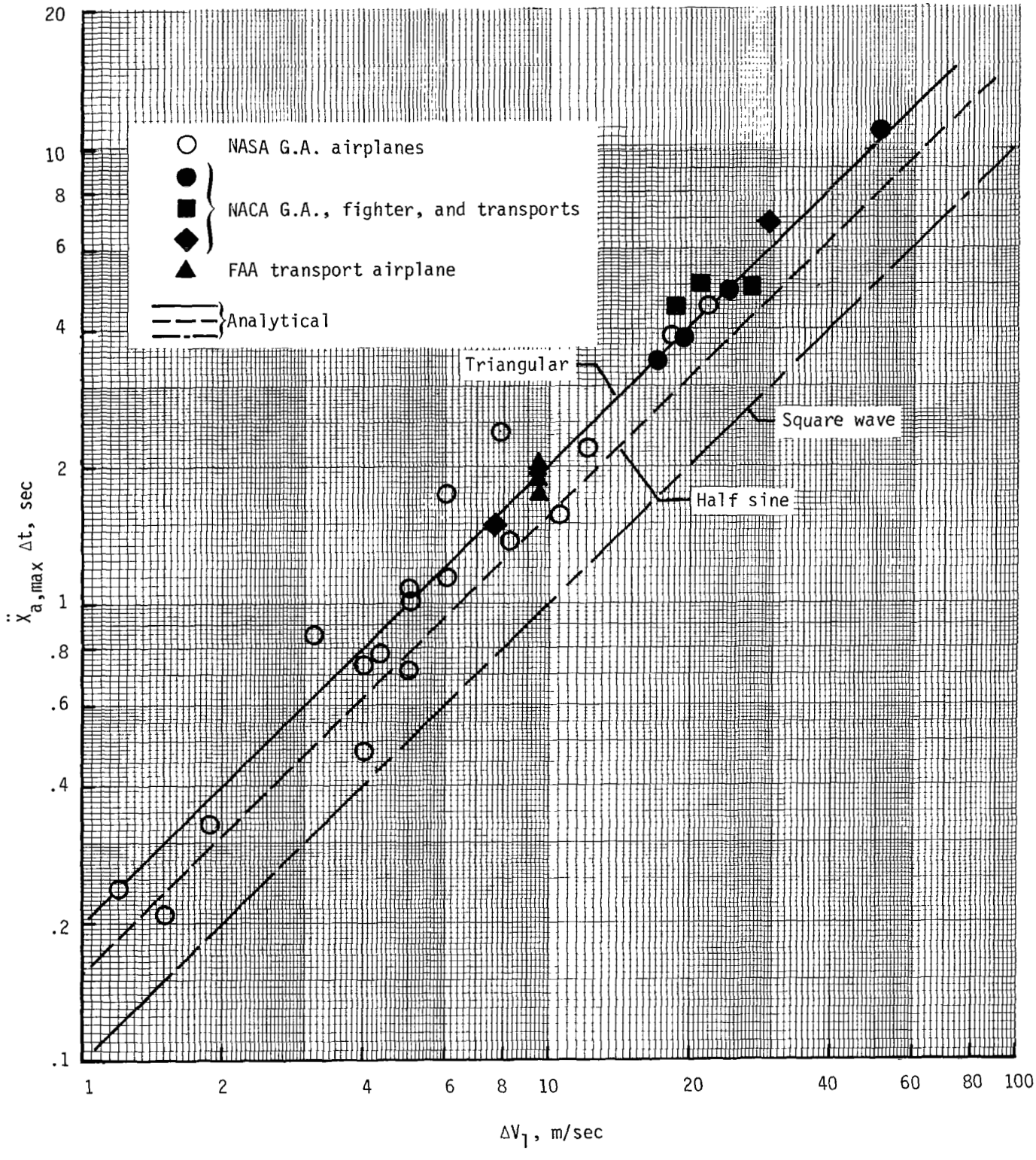

Figure 9.- Experimental and calculated longitudinal-impulse data for airplanes.

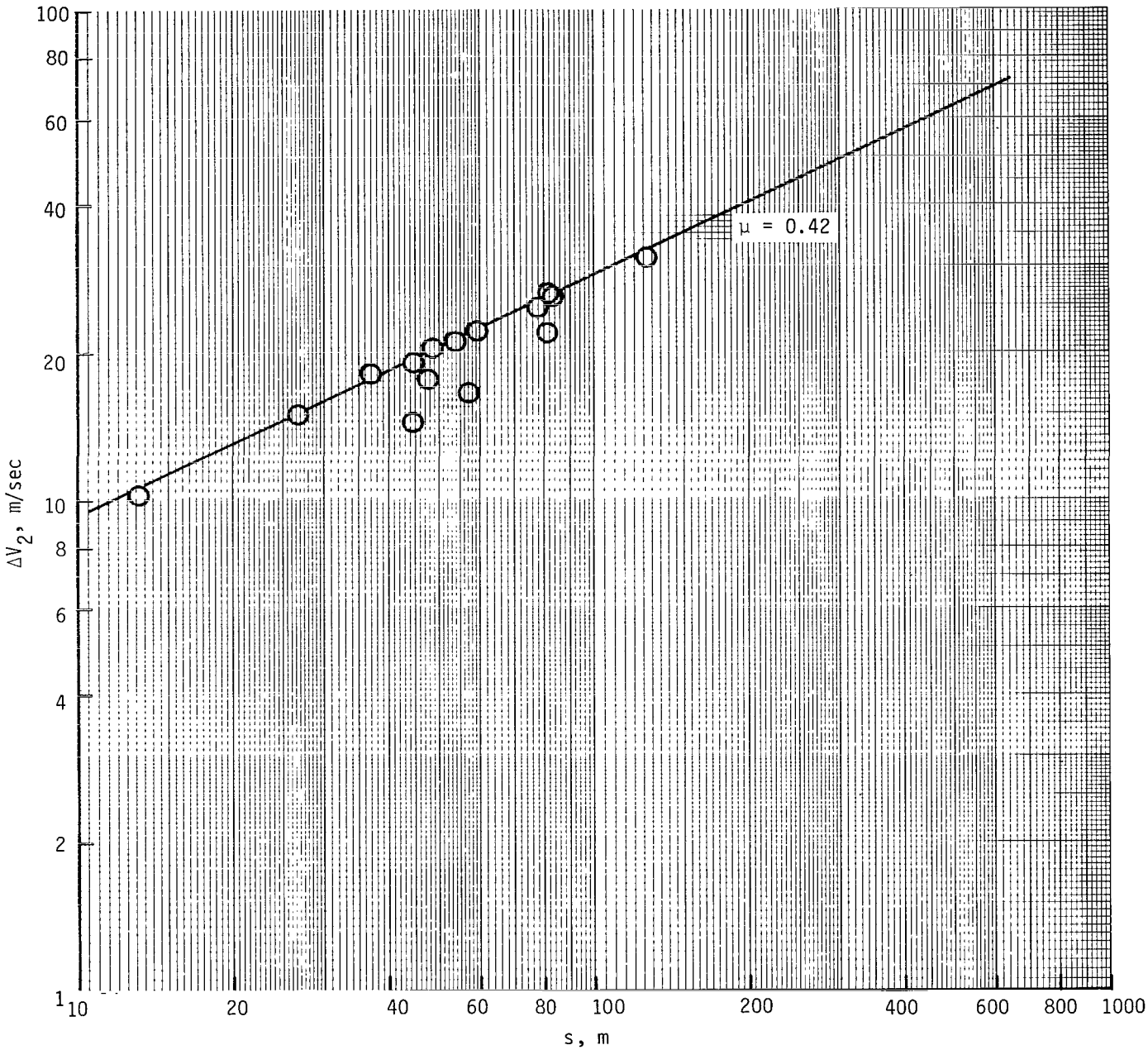

Figure 10.- Velocity change during slide-out plotted against slide-out distance.

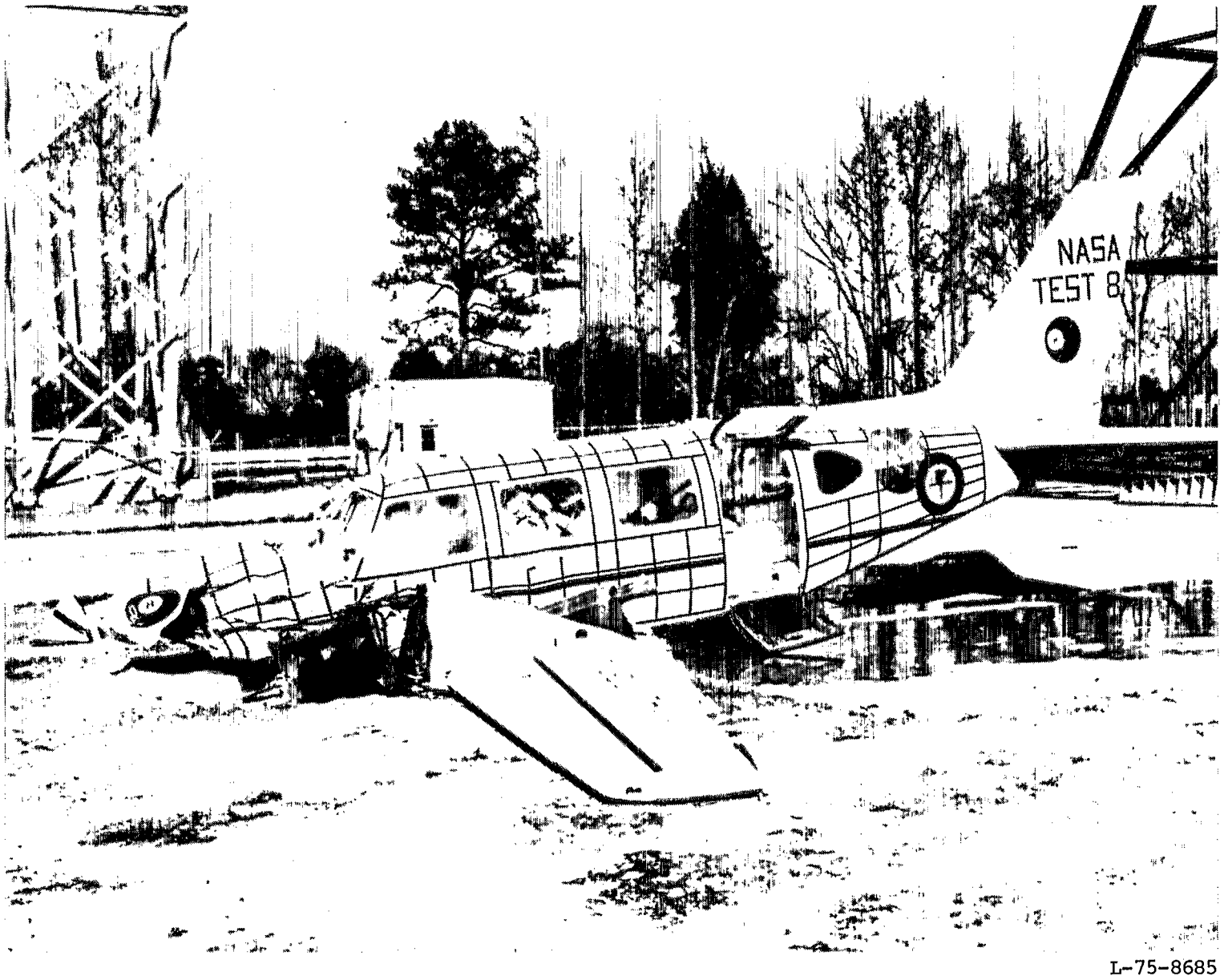

(a) Side view.

Figure 11.- Postcrash photographs of controlled crash test of a general aviation airplane.

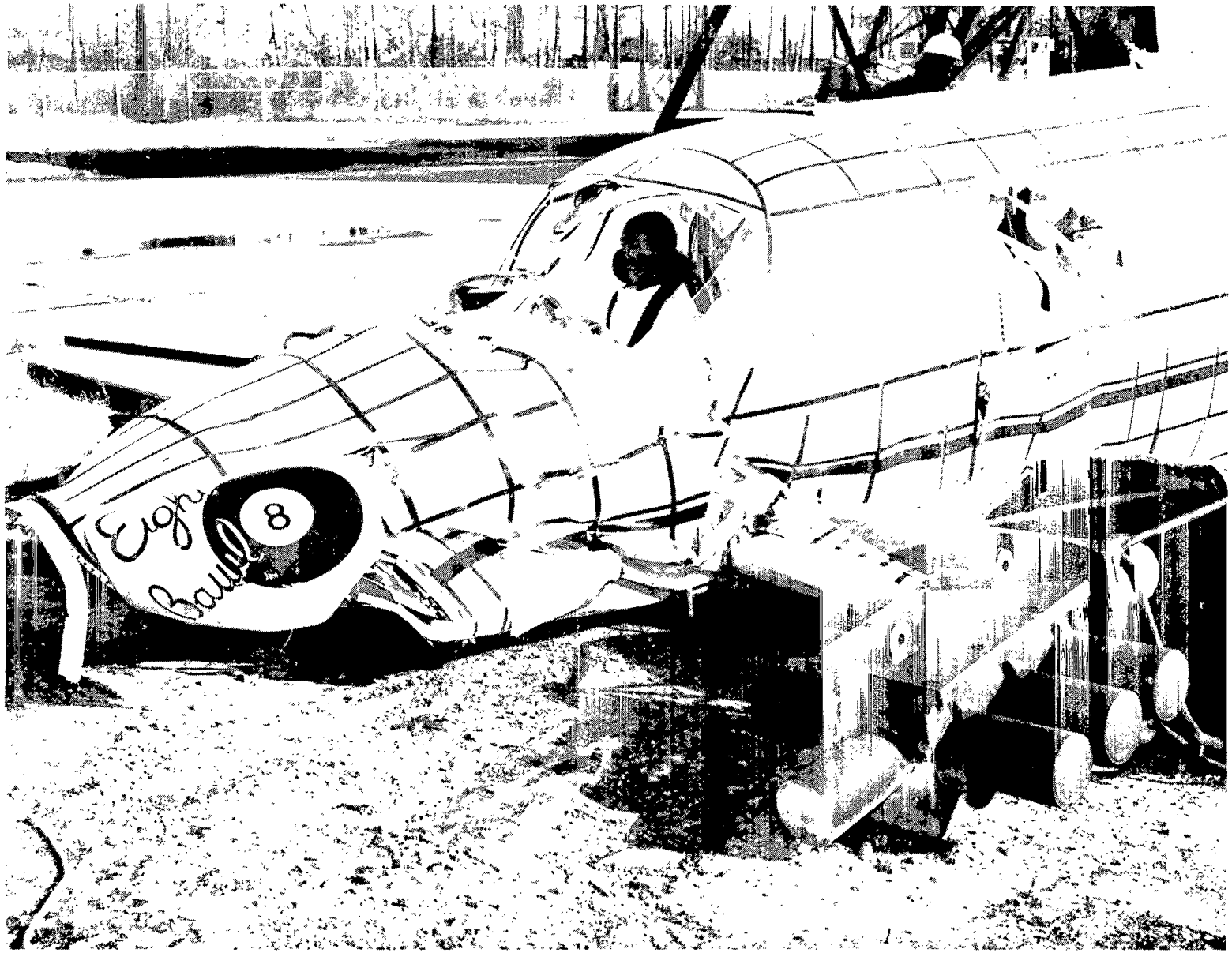

L-75-9116

(b) Three-quarter view of left side.

Figure 11.- Continued.

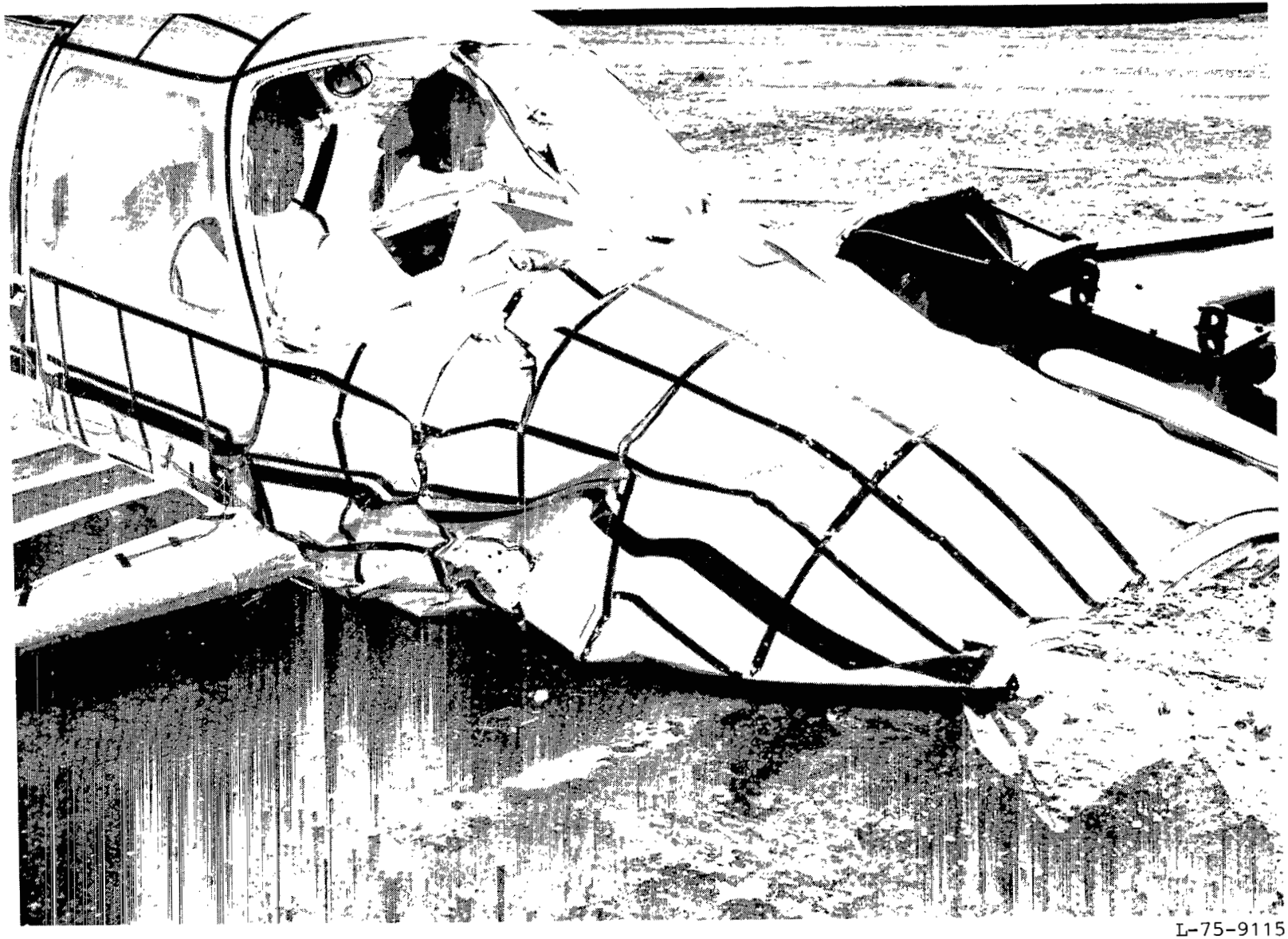

L-75-9115

(c) Three-quarter view of right side.

Figure 11.- Concluded.

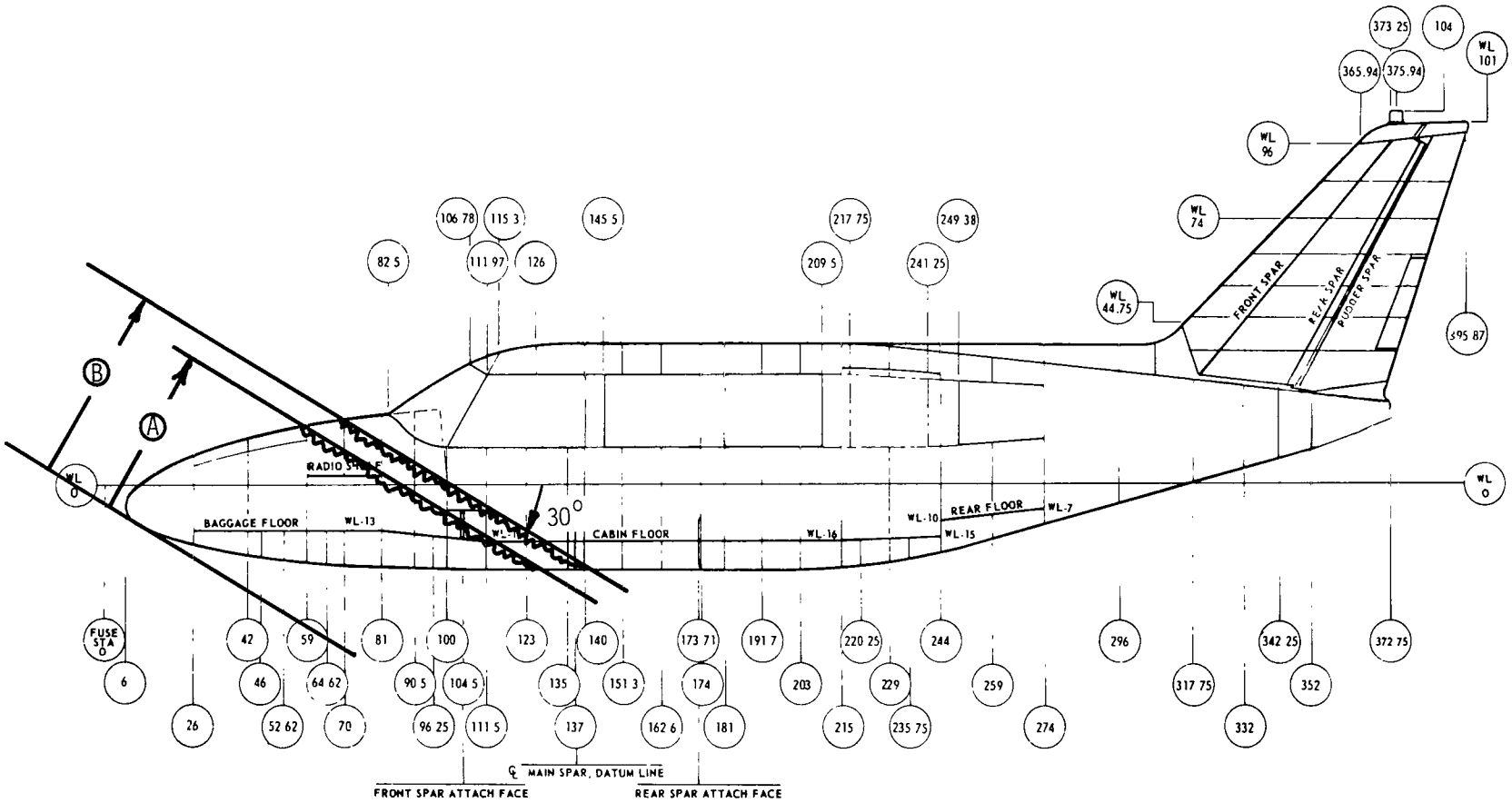

Measured crush on drawing		Scale factors	Crush distances
Ⓐ = 1.25 in.	Ⓑ = 1.45 in.	8.8/332 = Ⓐ/Z_A	Z_A = [(332) Ⓐ/8.8] [(0.3048/12)] 0.8 = 0.958 m
		8.8/332 = Ⓑ/Z_B	Z_B = [(332) Ⓑ/8.8] [(0.3048/12)] 0.8 = 1.112 m

Figure 12.- Airplane with station reference lines. All fuselage stations and water-line locations are given in inches. For consistency with the text, crush distances are given in meters.

1. Report No.	2. Government Accession No.	3. Recipient's Catalog No.
NASA TP-2083		

4. Title and Subtitle	5. Report Date
CORRELATION AND ASSESSMENT OF STRUCTURAL AIRPLANE CRASH DATA WITH FLIGHT PARAMETERS AT IMPACT	November 1982
	6. Performing Organization Code: 505-41-33-01
7. Author(s): Huey D. Carden	8. Performing Organization Report No.: L-15431
	10. Work Unit No.
9. Performing Organization Name and Address: NASA Langley Research Center, Hampton, VA 23665	11. Contract or Grant No.
	13. Type of Report and Period Covered: Technical Paper
12. Sponsoring Agency Name and Address: National Aeronautics and Space Administration, Washington, DC 20546	14. Sponsoring Agency Code

15. Supplementary Notes

16. Abstract

An analysis has been made of crash-deceleration pulse data from a crash-dynamics program on general aviation airplanes and from transport crash data available in the literature. This crash-dynamics program has been a joint effort since 1973 by the National Aeronautics and Space Administration (NASA) and the Federal Aviation Administration (FAA). The purpose of the analysis was to correlate and assess structural airplane crash data with flight parameters at impact. Uncoupled equations for the normal and longitudinal floor impulses (deceleration multiplied by duration) in the cabin area of the airplane were derived, and analytical expressions for structural crushing during impact and horizontal slide-out were also determined. Good agreement was found between experimental and analytical data for general aviation and transport airplanes over a relatively wide range of impact parameter. Two possible applications of the impulse data are presented: a postcrash evaluation of crash-test parameters and an assumed crash scenario. The data are believed to be of general significance regarding the assessment of expected loads at the seat/occupant structural interface for general aviation airplanes during serious but potentially survivable crashes.

17. Key Words (Suggested by Author(s))	18. Distribution Statement
Airplane crash tests Crash damage General aviation Impact tests Crash dynamics Impulse analysis	Unclassified - Unlimited Subject Category 39

19. Security Classif. (of this report)	20. Security Classif. (of this page)	21. No. of Pages	22. Price
Unclassified	Unclassified	42	A03

For sale by the National Technical Information Service, Springfield, Virginia 22161

NASA-Langley, 1982

1 1 1U,D, 821115 S00903DS
DEPT OF THE AIR FORCE
AF WEAPONS LABORATORY
ATTN: TECHNICAL LIBRARY (SUL)
KIRTLAND AFB NM 87117

S